AEROSPACE RESEARCH • AERODYNAMICS • PROPULSION • STRUCTURAL DYNAMICS • ELECTRONIC SYSTEMS AND INSTRUMENTS • COMPUTER MODULES

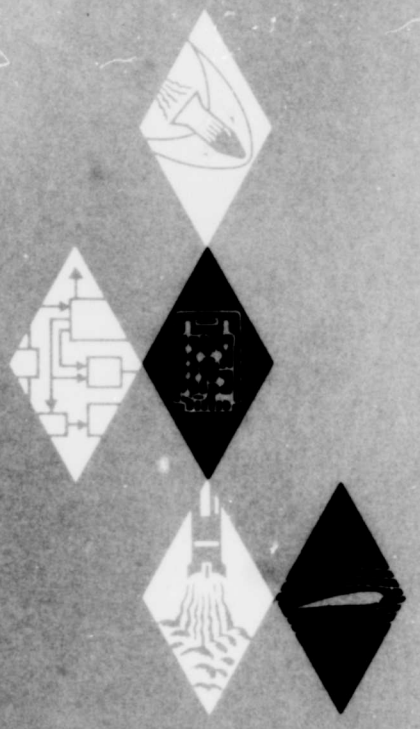

RESEARCH
ENGINEERING
PRODUCTION

TECHNICAL REPORT NO. 581

WIND TUNNEL INVESTIGATION OF THE TURBULENT NEAR WAKE OF A CONE AT ANGLE OF ATTACK

By A. J. Schlesinger
A. Martellucci

March 1966

GENERAL APPLIED SCIENCE LABORATORIES, INC.
MERRICK and STEWART AVENUES, WESTBURY, L.I., N.Y. · (516) ED 3-6960

Project 8030

Total No. of Pages - v and 55

Copy No. (10) of 125

TECHNICAL REPORT NO. 581

WIND TUNNEL INVESTIGATION OF THE TURBULENT NEAR WAKE OF A CONE AT ANGLE OF ATTACK*

By A. J. Schlesinger
A. Martellucci

Prepared for

Advanced Research Projects Agency
Washington 25, D. C.

Under Contract SD-149, Supplement #6
ARPA Order No. 396
Project Code 3790
"Ballistic Reentry Studies"

Project Engineer - H. Lien
Code 516 - ED 3-6960

Prepared by

General Applied Science Laboratories, Inc.
Merrick and Stewart Avenues
Westbury, L. I., New York

Approved by: Robert W. Byrne
Robert W. Byrne
Vice President

March 1966

*This research is sponsored by the Advanced Research Projects Agency

ABSTRACT

Aerodynamic measurements were made in the turbulent near wake of 10° half angle circular cone at a 10° angle of attack. The experiments were conducted at Mach 6 with a stagnation pressure of 800 psi and a corresponding free stream unit Reynolds number of 14.4 million per foot. The Reynolds number was sufficiently large so that the boundary layer at the cone shoulder was turbulent. Detailed radial profiles of the total and static pressures along the meridian plane of symmetry in the supersonic regions of the wake at several axial stations are presented. In addition, the shape of the u = 0 line in the meridian plane of symmetry was also obtained. Correlations are shown for near-wake data obtained for zero angle of attack.

TABLE OF CONTENTS

LIST OF FIGURES

LIST OF FIGURES

BLANK PAGE

TECHNICAL REPORT NO. 581

WIND TUNNEL INVESTIGATION OF THE TURBULENT NEAR WAKE OF A CONE AT ANGLE OF ATTACK

By A. J. Schlesinger
A. Martellucci

I. INTRODUCTION

The problem of identifying a vehicle from wake observables has become more complex as a result of the use of lifting type bodies as reentry vehicles. These vehicles have asymmetric flow fields about them due to body geometry (viz., elliptic cone) or flight attitude which cause three-dimensional effects from the body flow to enter the wake. In general, reentry vehicles will experience a sequence of damped oscillations in their downward trajectories which also effect the wake. Therefore, to provide a better correlation between the wake observables and vehicle characteristics it is necessary to have estimates of the effects of three-dimensionality in the wake.

Near wake data have been obtained by several investigators for circular cones at zero angle of attack (Refs. 1 and 2). Near wake characteristics of an elliptic cone at zero angle of

attack have also been obtained and the effects on the wake properties are discussed in detail in Ref. 3.

The present test program deals with the effects of flight attitude on the near wake. It is purely fluid mechanical in nature and no attempt is made to consider the effects of chemistry in the problem. The experiments were conducted in General Applied Science Laboratories Mach 6 Blow-Down Facility. Measurements of the base pressure, cone surface pressures, boundary layer pitot profiles at the cone shoulder, axial and radial distributions of the stagnation and static pressure in the supersonic portions of the near wake and the "u = 0" line of the recirculation region have been obtained for 10° half angle circular cone with a 5.12" base diameter at 10° angle of attack. Tests were conducted in a Mach 6 stream at a stagnation pressure of 800 psia and a corresponding free stream unit Reynolds number of 14.4×10^{6} per foot.

II. EXPERIMENTAL FACILITY

The test program was performed in a contoured Mach 6 axisymmetric nozzle with a 12-inch diameter test section. The nozzle was connected to the GASL Blow-Down Facility which is capable of delivering air at a maximum temperature of 1200°R and at a maximum pressure of 1500 psi. The nozzle exhausted into a 40-foot diameter vacuum sphere which was evacuated to a pressure of 10 to 25 mm of mercury prior to each test. Due to the loads exerted on the model caused by the starting process, actuating rods were used as additional supports for the model. These rods were retracted from the model and flow field when steady-state conditions were achieved. A complete description of the facility and equipment used for this test program is presented in Ref. 4.

III. MODEL AND INSTRUMENTATION

The basic model tested was a 10° half angle blunted cone with a nose radius of 0.125 inches and a base diameter of 5.12 inches. The model was placed in the test section at 10° angle of attack.

A. Description of Model

The support system utilized in this test series consisted of a towing wire and three stainless steel struts. The towing wire supports the model at its vertex and extends upstream through the nozzle throat. It is a stainless steel cable, 0.125" diameter. The model is supported at its base by three stainless steel struts in the form of double wedges 0.0625" thick and 0.500" wide with a 20° included wedge angle and are swept back 60°. The towing wire is kept under tension by a spring mechanism located outside of the tunnel. The struts are hollowed to allow instrumentation wires to pass out of the tunnel. A schematic of this support system is shown in Fig. 1 and a photograph of the model mounted in the test section is shown in Fig. 2.

B. Instrumentation

1. Pitot-Cone Rake

The flow properties in the supersonic portion of the wake were recorded by means of a pitot-cone rake shown in Fig. 3. This rake consists of seven 7.5° half angle cone probes. The accuracy of the probe tips were checked with an optical comparator and the cone angle was found to be 7.5° ± 0.2°. Two static pressure taps were located 20 nose diameters from the apex and are 180° apart. The centerline of these holes is perpendicular to the cone vertical meridian plane, which minimizes the crossflow effect. This probe measured the pitot pressure in the wake as well as the cone static pressure.

2. Base Pressure

The base pressure was measured at the center of the base.

3. u = 0 Probe

The probe used to measure the location of the "u = 0" line was reported in Ref. 1. A schematic of the probe is shown in Fig. 4. The probe was located at a prescribed axial station behind the model and was moved radially during the test. The point where u = 0 corresponds to the location

of zero axial pressure differential. The base pressure was recorded for all tests where the probe was extended into the recirculation region. The base pressure was unaffected by the presence of the probe.

4. Surface Pressure

To determine the surface pressures, a base supported model was used. Static taps were located on the surface of the cone at 30° intervals. Instrumentation tubes were passed through the base of the model and out of the tunnel.

5. Boundary Layer Probe

To determine the pitot pressures in the boundary layer at the cone shoulder the probe shown in Fig. 5 was used. The probe was actuated across the boundary layer during a test.

6. Transducers and Recorder System

The transducer output was recorded on both Sanborn and Visicorder Oscillograph recorders. A single, continuous trace 0-0.50 psia CEC transducer was employed for base pressure measurements. The pitot pressures and cone static pressures were recorded with a model 48D3 Scanivalve, designed for low pressure measurements. To determine the "u = 0" line a ± 2.50 psi differential transducer was used.

IV. RESULTS AND DISCUSSION

The work presented in this report represents a continuation of the experimental studies to determine the effects of three-dimensionality of wake observables under development at GASL. A circular cone at angle of attack was chosen as a model to determine the effect of flight attitude because it represents a lifting configuration and the flow about the cone is amenable to analysis. The initial conditions for the near wake development are dependent on the flow properties, both viscid and inviscid, at the shoulder of the body prior to the expansion into the base region. Therefore, the first part of the experimental investigation was devoted to measuring the properties at the shoulder of the model. The second part of the investigation was to determine the flow properties in the supersonic portion of the near wake.

The experimental program was carried out on a 10° half angle cone at 10° angle of attack. The free stream Mach number was 6.02, the stagnation pressure was 800 psia. These conditions correspond to a test section unit Reynold's number of 14.4×10^{6} per foot.

A. Flow About Right Circular Cone at Angle of Attack

The surface pressure distribution about the right

circular cone at angle of attack was measured and is shown in Fig. 6 along with the pressure distribution computed by the tangent cone method (Ref. 6). It can be seen that the experimental results compare well with theory. Figures 7 and 8 show the streamline patterns on the model using lampblack as an indicator. It is clear from these photographs that the tow wire system does not influence, to any observable extent, the flow over the cone.

In addition to the surface pressure distribution, the boundary layer pitot pressures were measured both on the windward and leeward sides of the cone. The pitot pressure distributions are shown in Figs. 9 and 10 respectively. The boundary layer thickness derived from the turbulent analysis of Reshotko and Tucker (Ref. 5) for a 10° half angle cone at zero angle of attack is also included.

B. Evaluation of the Compression Strut Support

Because the tow-rod band support system reported in Ref. 1 could not be adopted to support a model at an angle of attack, an alternative support system was considered. This support consists of three slender base struts as shown in Fig. 11. To establish whether the support would be as efficient as the tow-rod band support system, measurements of the

u = 0 line and also the centerline Mach number at a station X/D = 2.0 were measured. The u = 0 line obtained with the strut-wire support and also the tow-rod band support that were reported in Ref. 1 are shown in Fig. 12. Also shown are three points measured for the present system. The centerline Mach number distributions of the strut-wire and tow-rod band support are shown in Fig. 13 along with the measured value at X/D = 2.0 for the present support. It is clear from Figs. 12 and 13 that the compression strut support provide a system that is equivalent to the tow-rod band support reported by GASL in Ref. 1.

C. Near Wake Data

The base pressure on the circular cone at angle of attack was measured with 0-0.5 psia CEC transducers located inside the model. The base pressure was measured at the centerline of the base. The pressure level recorded was lower than that for a circular cone at zero angle of attack. This base pressure was used as a guide in the determination of the u = 0 line. That is, a sudden change in the level of the base pressure, while probing with the u = 0 probe, would indicate a change in the structure of the wake due to the presence of the probe. However, for all of the data obtained in the

recirculation region, the base pressure was unaffected. The "u = 0" line was obtained and is shown in Fig. 14. It is interesting to note the shape of the "u = 0" line on the windward side of the model. The slope of the line referred to the wind axis is much greater on the windward side as compared to the leeward side, indicating that a shift of the profiles toward the leeward side in the near wake is to be expected. The downstream stagnation point was found to be at an axial station of $X/D \cong 0.78$.

The pitot pressure and cone probe pressure in the supersonic regions of the wake were recorded with the multiple rake shown in Fig. 3. The radial distributions of pitot pressure and cone static pressure for each axial station are shown in Figs. 15A to 15G and Figs. 16A to 16G respectively. The base centerline is included as a reference line for comparison with zero angle of attack. The profiles as shown on the graph are shifted toward the leeward side of the cone. The radial distribution (i.e. perpendicular to the wind axis) of Mach number for each axial station, computed from the measured cone probe and pitot pressures are shown in Figs. 17A to 17G. The location of the trailing shock was obtained from the

pressure measurements and was verified from shadowgraphs of the wake. The axial shape of the trailing shock in the meridian plane of symmetry is shown in Fig. 14.

V. COMPARISON OF ANGLE OF ATTACK WAKE WITH ZERO ANGLE OF ATTACK DATA (REF. 1)

The u = 0 line and shock shape for the circular cone at zero angle of attack and a 10° angle of attack are shown in Fig. 14. As can be seen, the u = 0 line and shock shape for the cone at angle of attack are shifted toward the leeward side of the cone. The rear stagnation point for the zero angle of attack cone is at X/D ≅ 0.78. Typical radial distributions of pitot pressures at several axial stations for both cases are shown in Figs. 18 to 20. The centerline for the zero angle of attack case is used as a reference. Here again it can be seen that the profiles for the angle of attack case are shifted toward the leeward or low pressure side. A comparison of the static pressure distributions in the near wake is shown in Fig. 21; the centerline values are used for the zero angle of attack case and the minimum values of the profiles are used for the angle of attack case. For the zero angle of attack case there is an overcompression to p/p_∞ of 1.6 before the flow overexpands to a static pressure less than p_∞ at X/D ≈ 2.5 whereas in the 10° angle of attack case and also for the elliptic cone at zero angle of attack the increased mixing due to the flow asymmetry flattens the distribution. The nominal static pressure level is approximately

p_∞ and there are indications of a slight positive gradient.

The total pressure distribution at the minimum points of the radial profiles for both cases are also shown in Fig. 21. The total pressure in the near wake region for the angle of attack case is substantially larger than that for the zero angle of attack wake.

VI. CONCLUDING REMARKS

An experimental investigation has been conducted to determine the fluid mechanical properties of the turbulent near wake of a cone at angle of attack in a hypersonic stream. Tests were run at a Reynolds number that was sufficiently large to insure a turbulent boundary layer at the cone shoulder. Information necessary to assess the physical properties and structure of the asymmetric wake of a 10° half angle cone at a 10° angle of attack in Mach 6 stream have been obtained. The tests were conducted at a stagnation pressure of 800 psia with a corresponding Reynolds number referred to the base diameter of 6.15×10^{6}. The model was supported by a nose tow wire and three slender swept struts from the base.

The following are the principal results of the data obtained:

1. The location of the downstream stagnation point was determined from the u = 0 line measurement. The stagnation point was located at X/D = 0.78 from the model base.

2. The u = 0 line was distorted from the zero angle of attack shape and was shifted toward the leeward or low pressure side.

3. There was a shift in the pitot pressure and cone probe pressure profiles toward the leeward side of the cone.

4. The static pressure in the supersonic portion of the near wake did not experience an overcompression as was the case for the cone at zero angle of attack. However, the static pressure experiences a slight positive gradient.

5. The stagnation pressure in the supersonic region of the near wake ($1.25 \leq X/D \leq 2.50$) was observed to be much larger than for either the zero angle of attack case or the elliptic cone case.

6. The trailing shock shape, obtained with pitot pressure measurements and confirmed by shadowgraph pictures, shifted toward the leeward or low pressure side.

VII. REFERENCES

1. Martellucci, A., Trucco, H., and Agnone, A., Measurements of the Turbulent Near Wake of a Cone at Mach 6, GASL TR-482, December 1964.

2. Zakkay, V. and Cresci, R. J., An Experimental Investigation of the Near Wake of a Slender Cone at M_∞ = 8 and 12, ARL 65-87, May 1965.

3. Trucco, H., Martellucci, A., Ranlet, J., and Agnone, A., Measurements of the Turbulent Near Wake of an Elliptic Cone at Mach 6, GASL TR-537, September 1965.

4. Anon., Description of Experimental Facility, GASL, November 16, 1965.

5. Reshotko, E. and Tucker, M., Approximate Calculation of the Compressible Turbulent Boundary Layer with Heat Transfer and Arbitrary Pressure Gradient, NACA TN 4154, December 1957.

6. Hays, W. D. and Probstein, R. F., Hypersonic Flow Theory, Academic Press, New York, 1959.

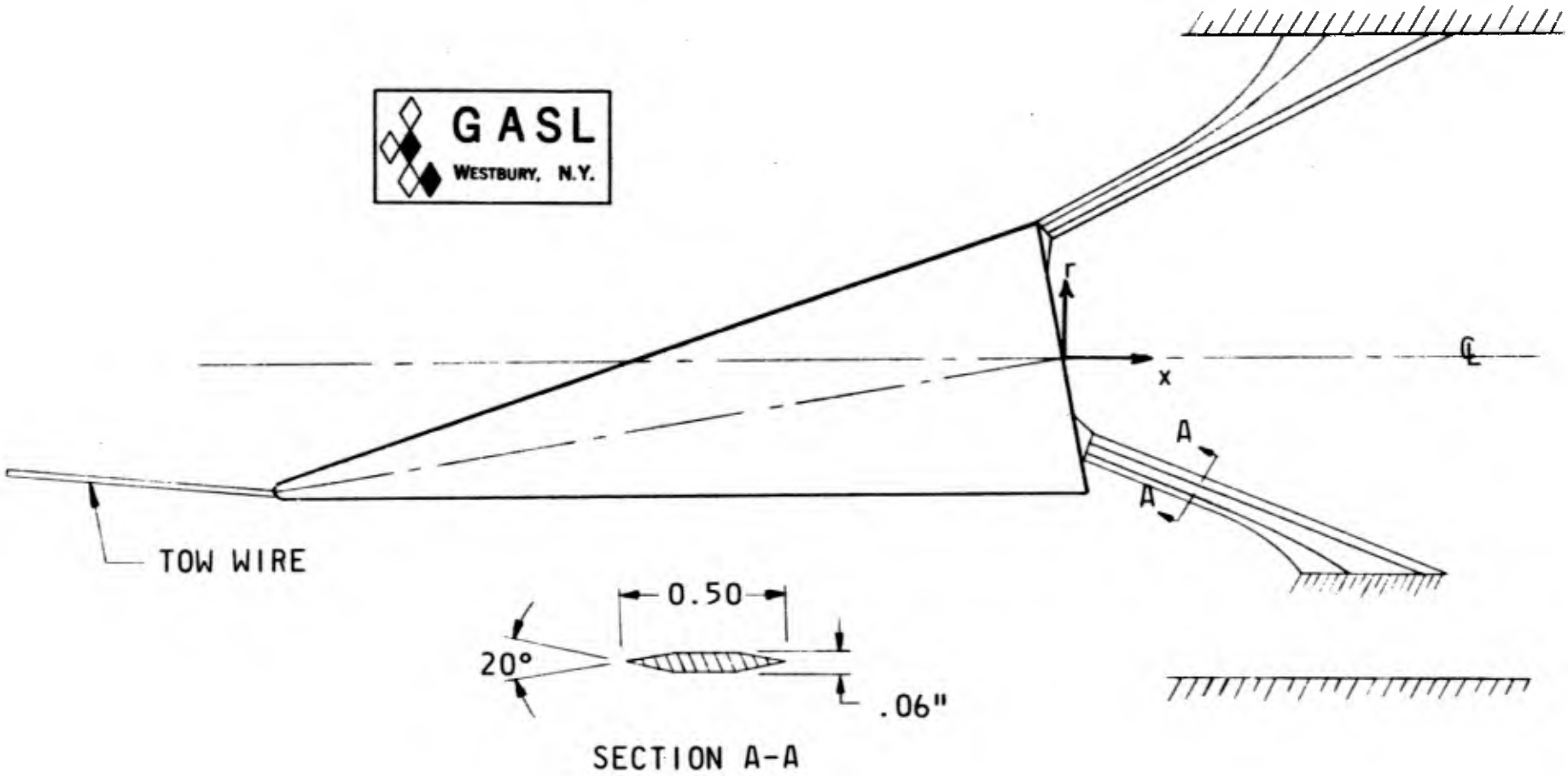

FIGURE 1: SCHEMATIC OF SUPPORT SYSTEM

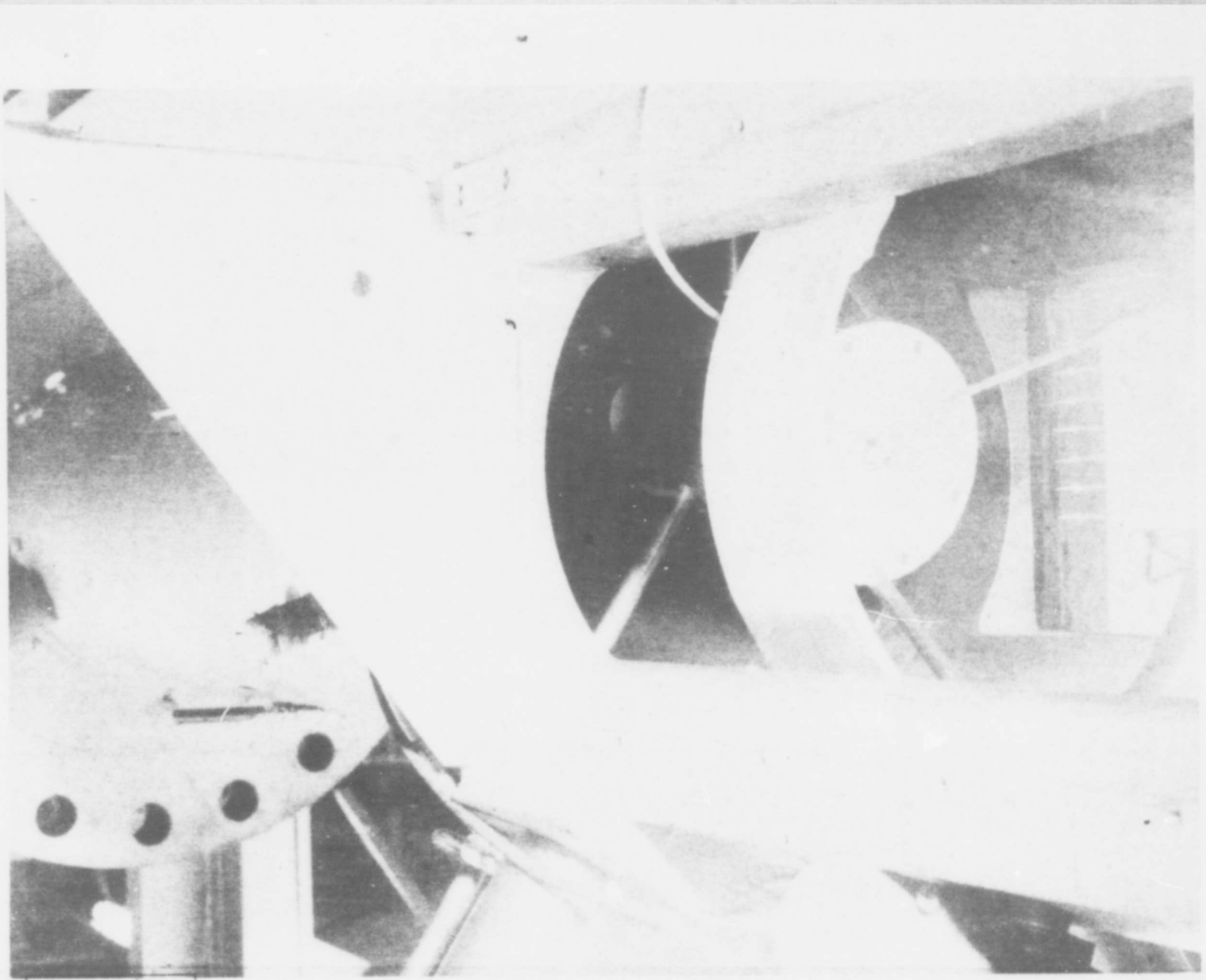

GASL
WESTBURY, N.Y.

FIGURE 2. MODEL IN TUNNEL (Starting Strut Extended)

FIGURE 2: MODEL IN TUNNEL (Starting Strut Extended)

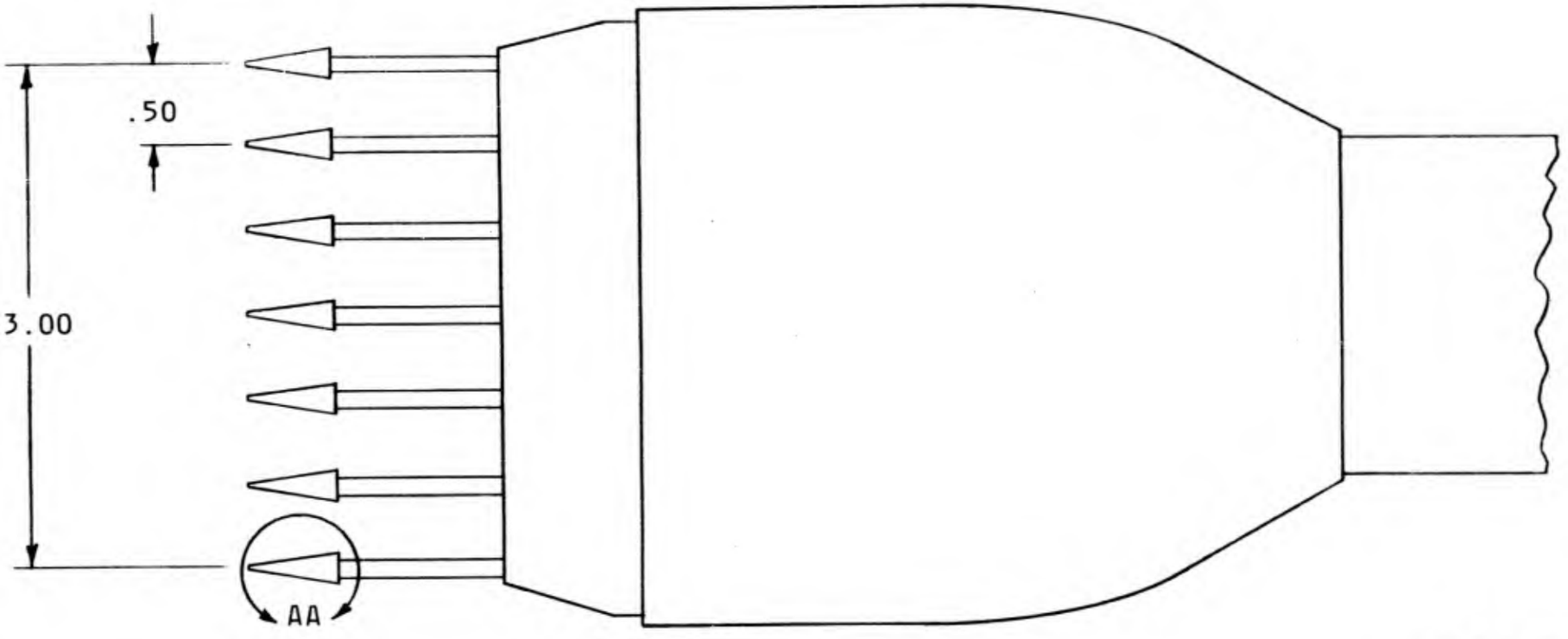

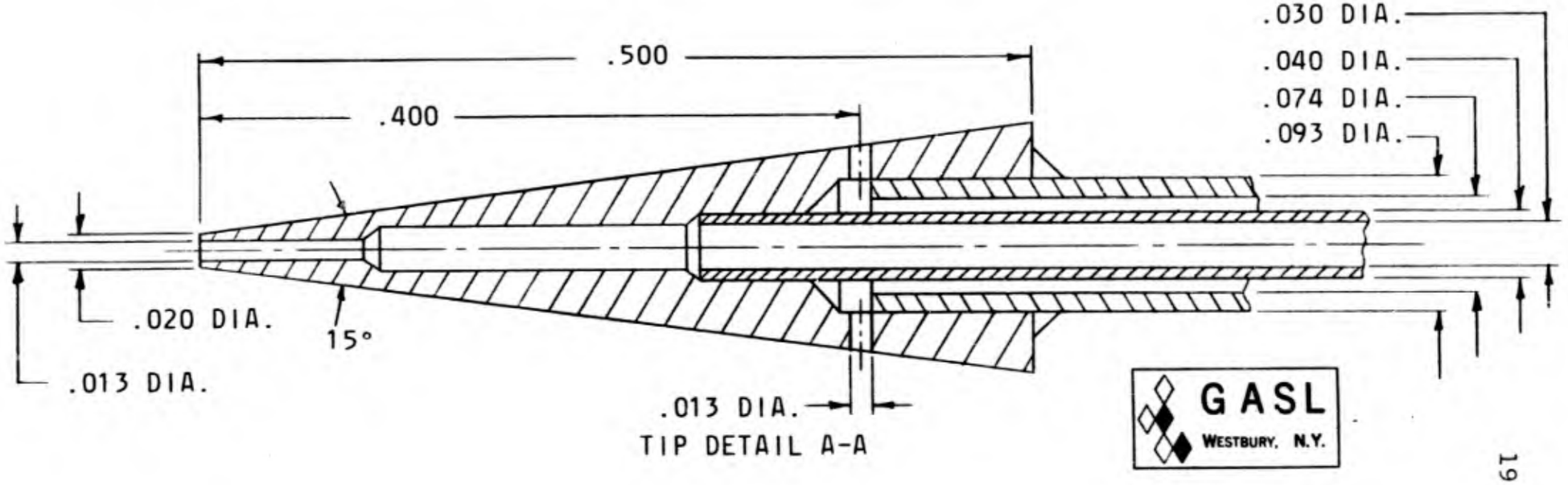

FIGURE 3: PITOT - CONE RAKE

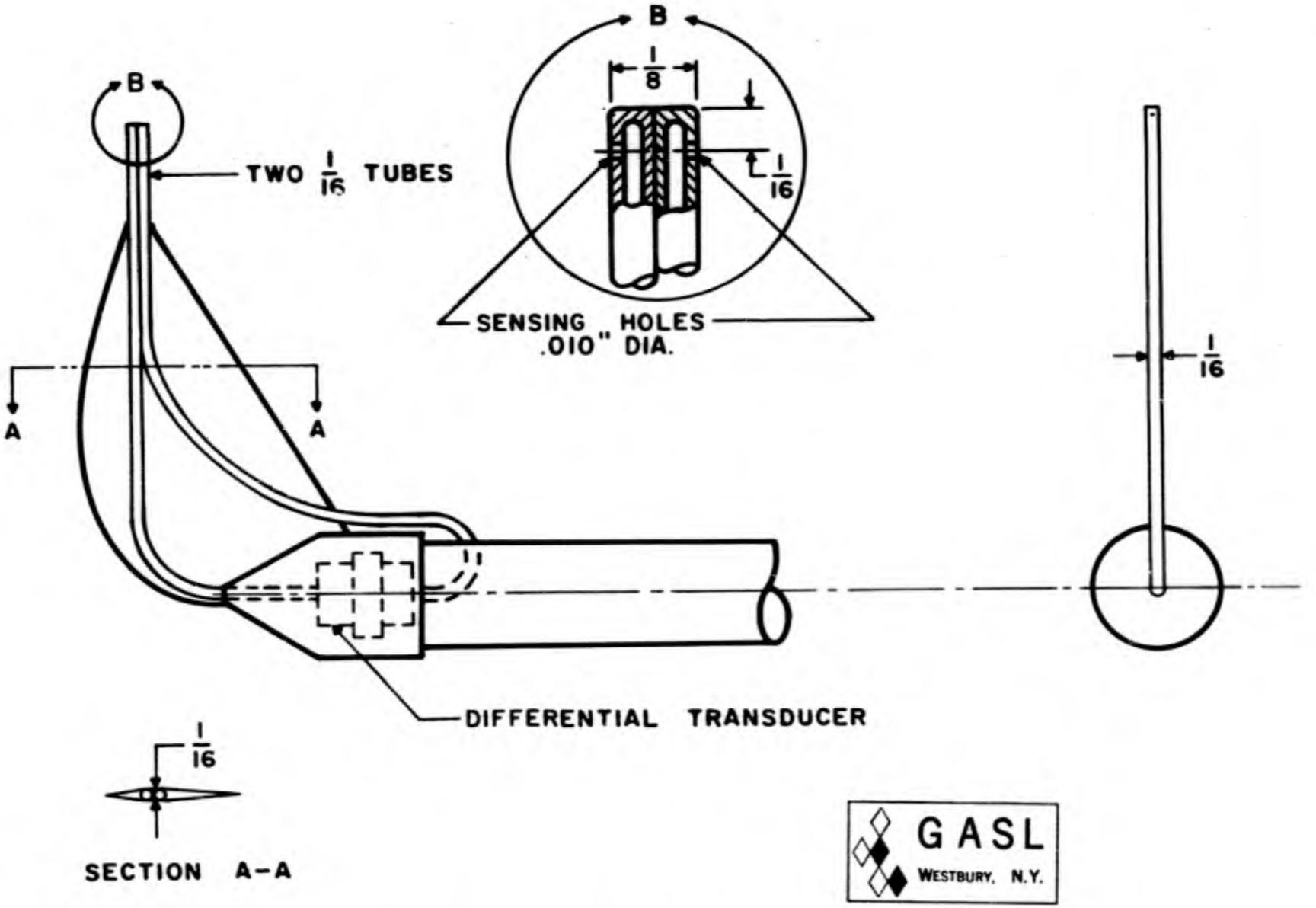

FIG. 4 u=0 PROBE

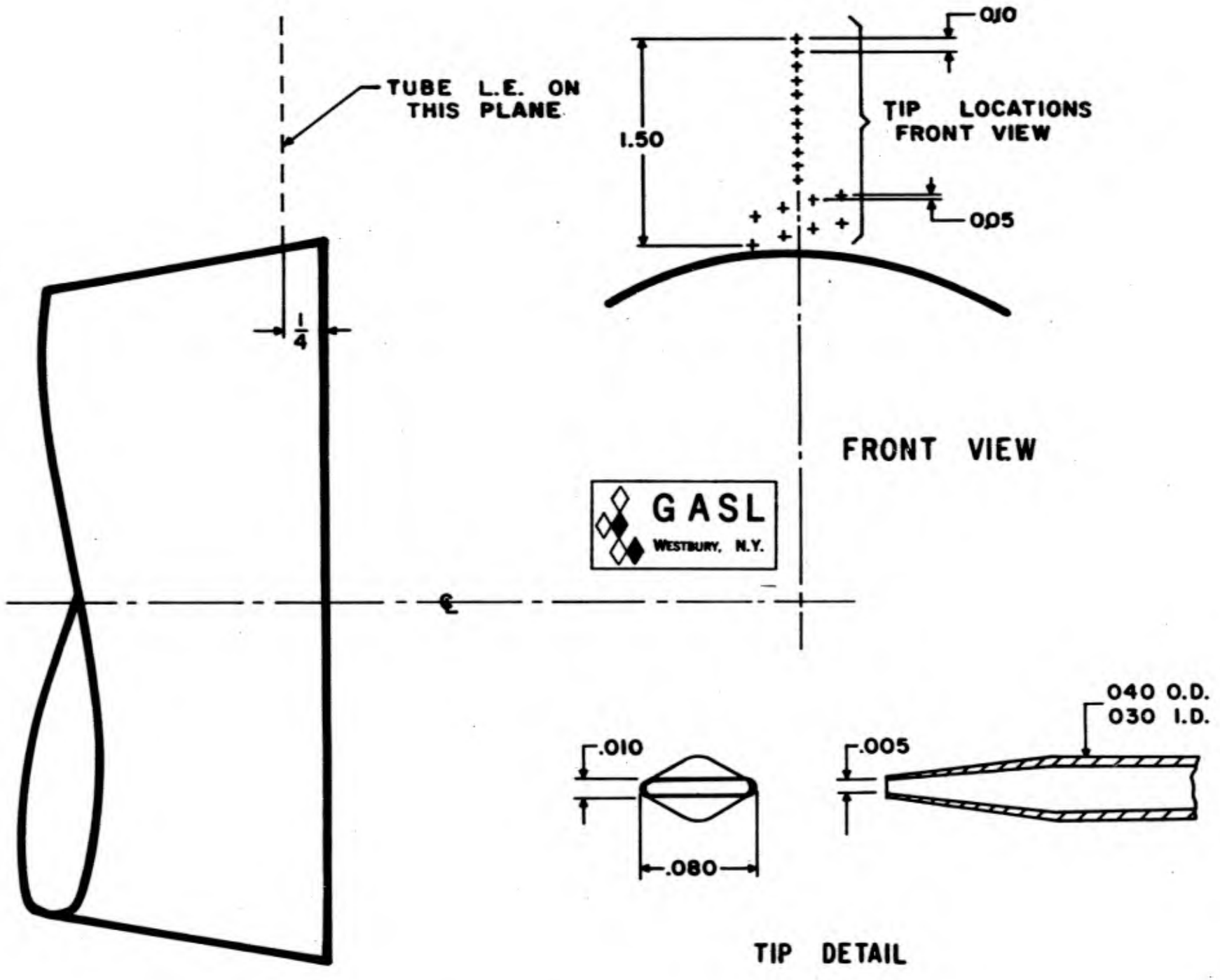

FIG. 5 BOUNDARY LAYER RAKE

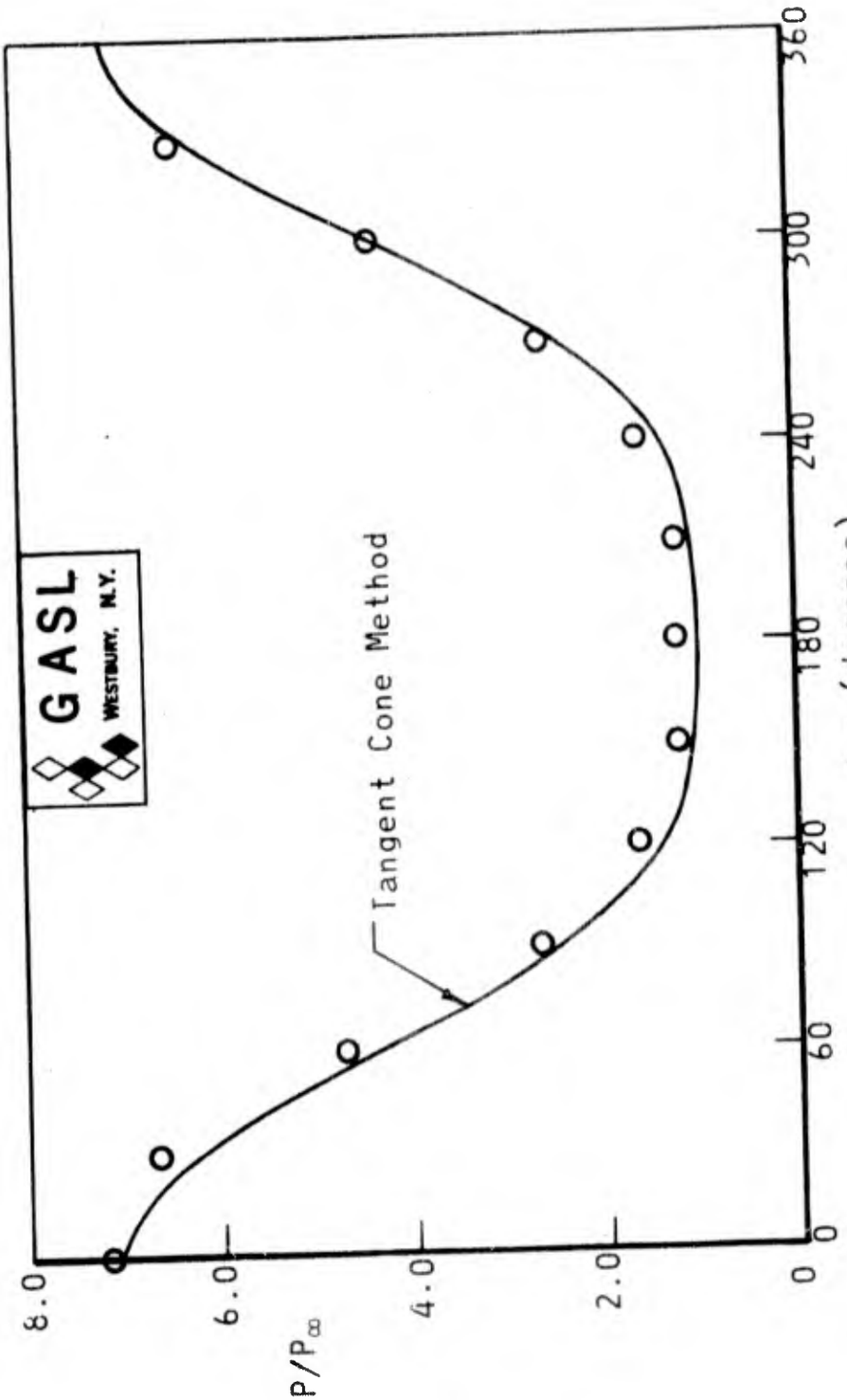

FIGURE 6: SURFACE PRESSURE DISTRIBUTION

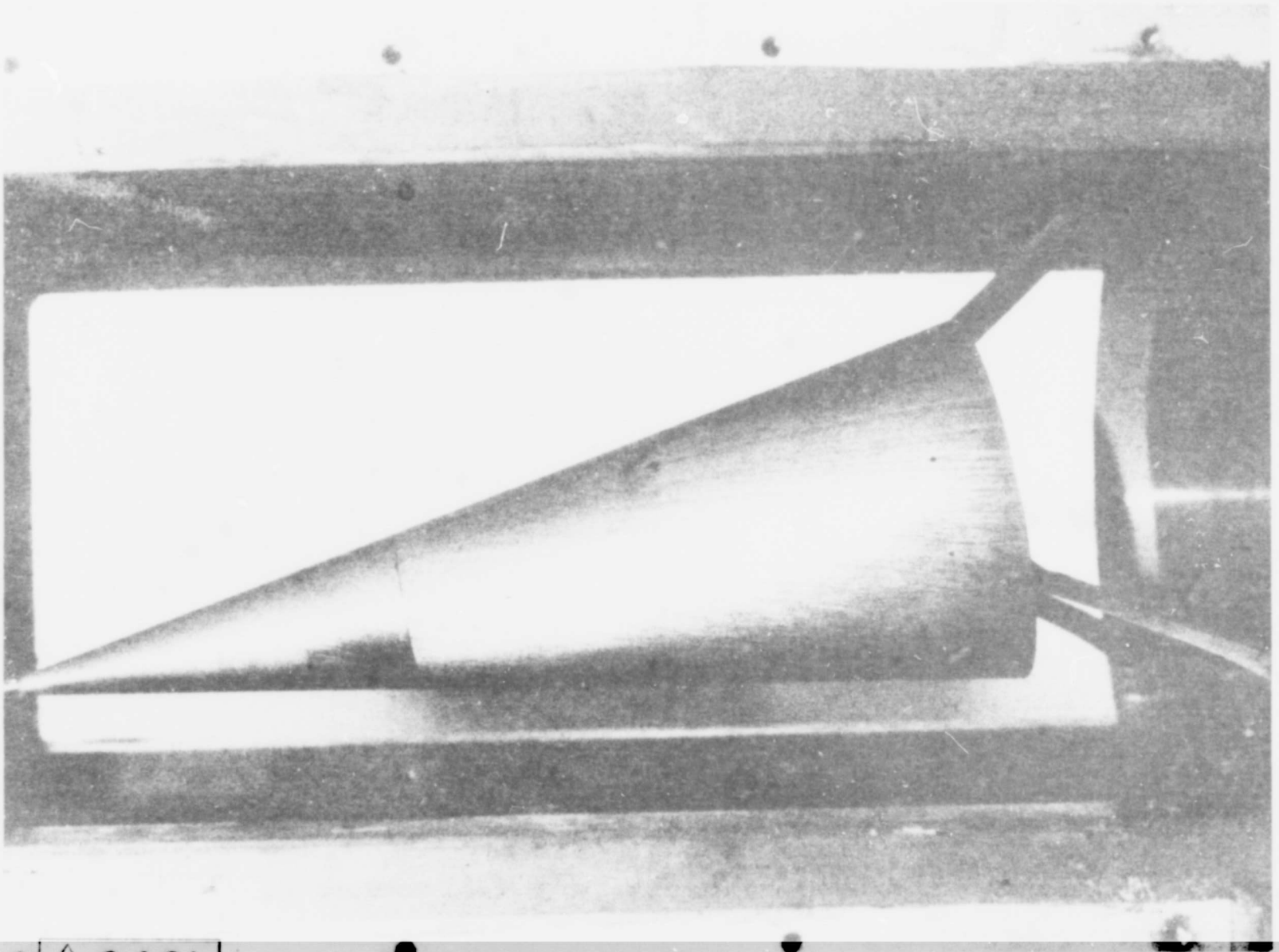

GASL
WESTBURY, N.Y.

FIGURE 7: MODEL SHOWING STREAMLINES (View from Side)

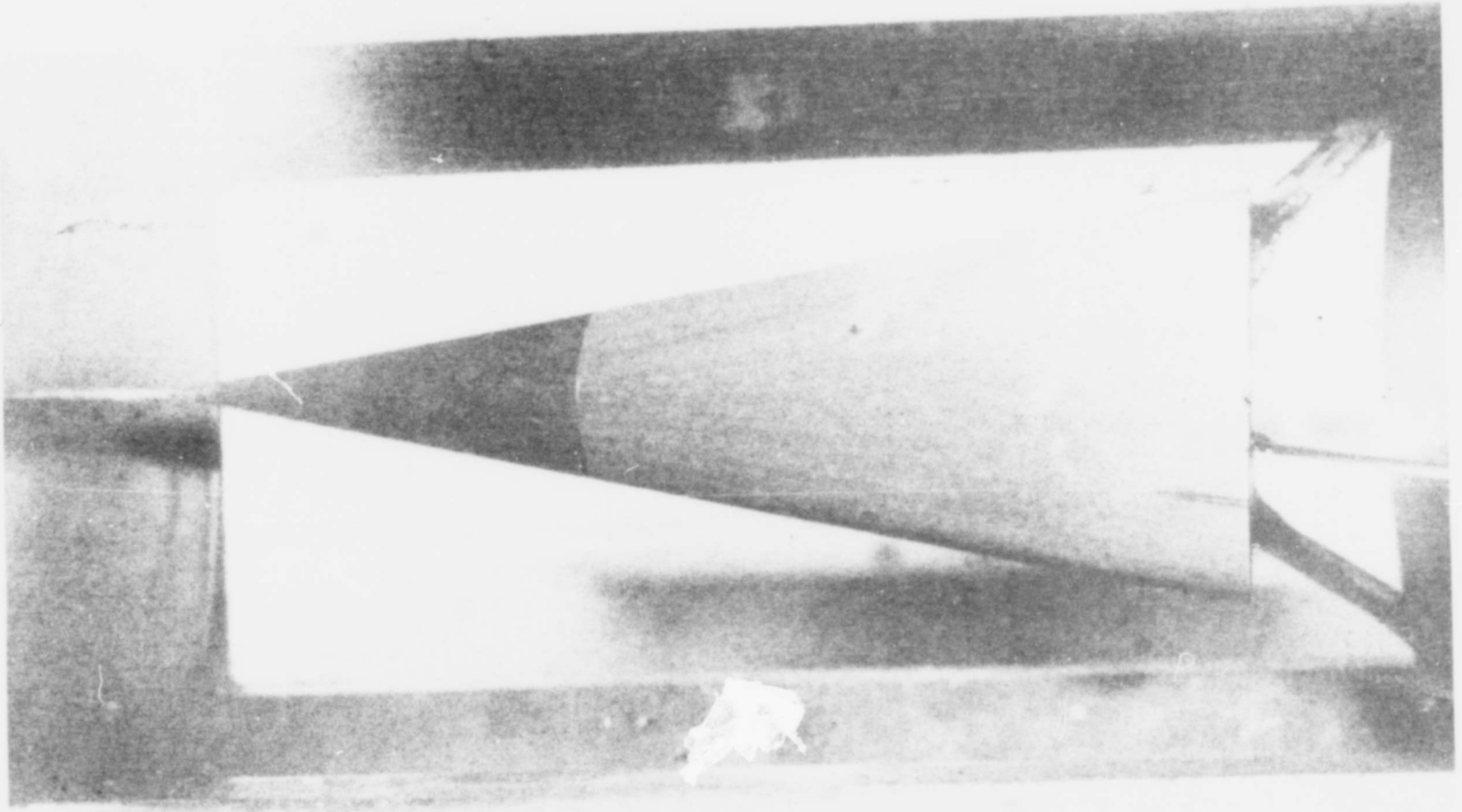

GASL
WESTBURY, N.Y.

FIGURE 6: MODEL SHOWING STREAMLINES (Viewed from Windward)

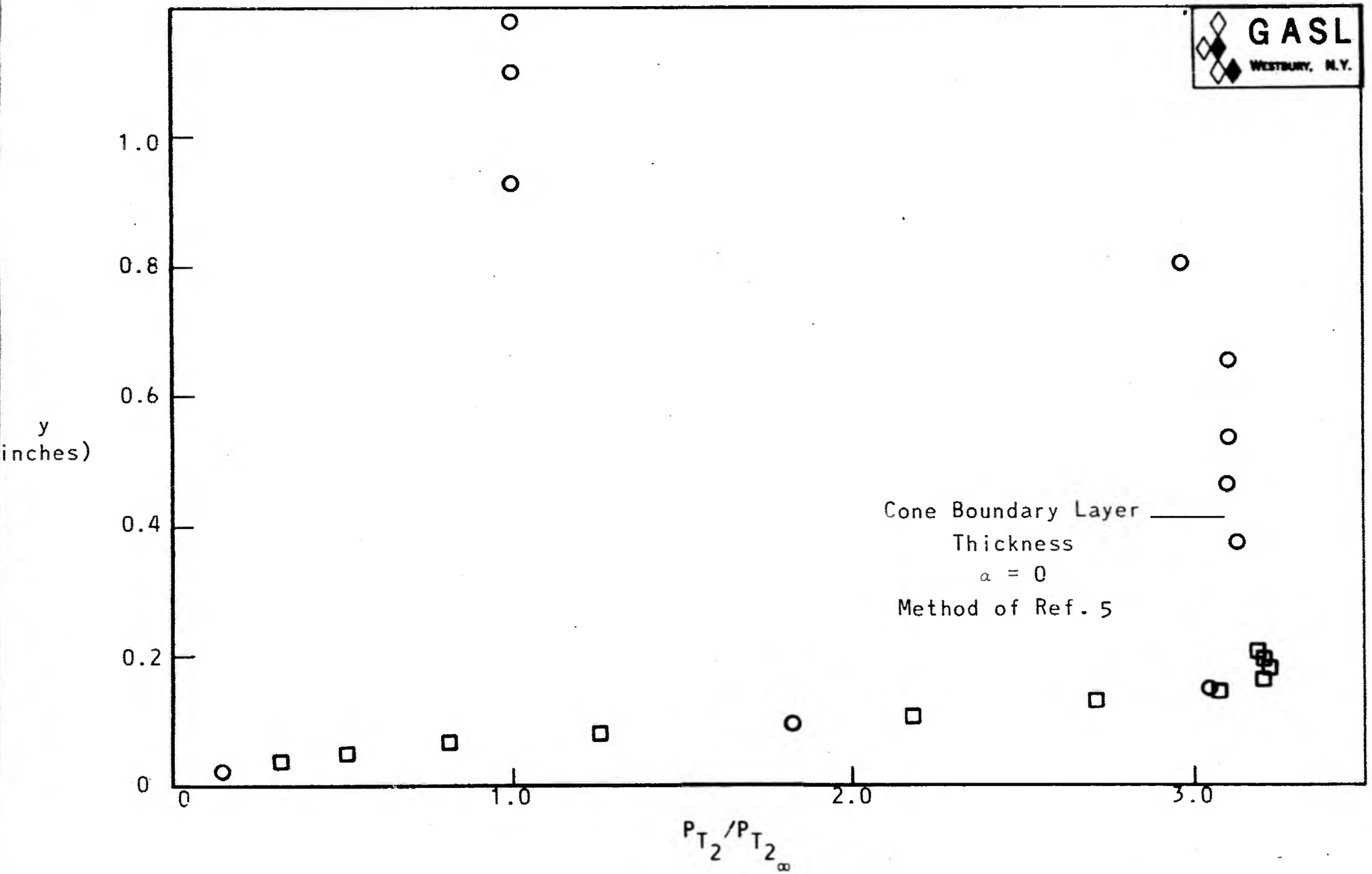

FIGURE 9: BOUNDARY LAYER PITOT PROFILE AT CONE SHOULDER WINDWARD SIDE

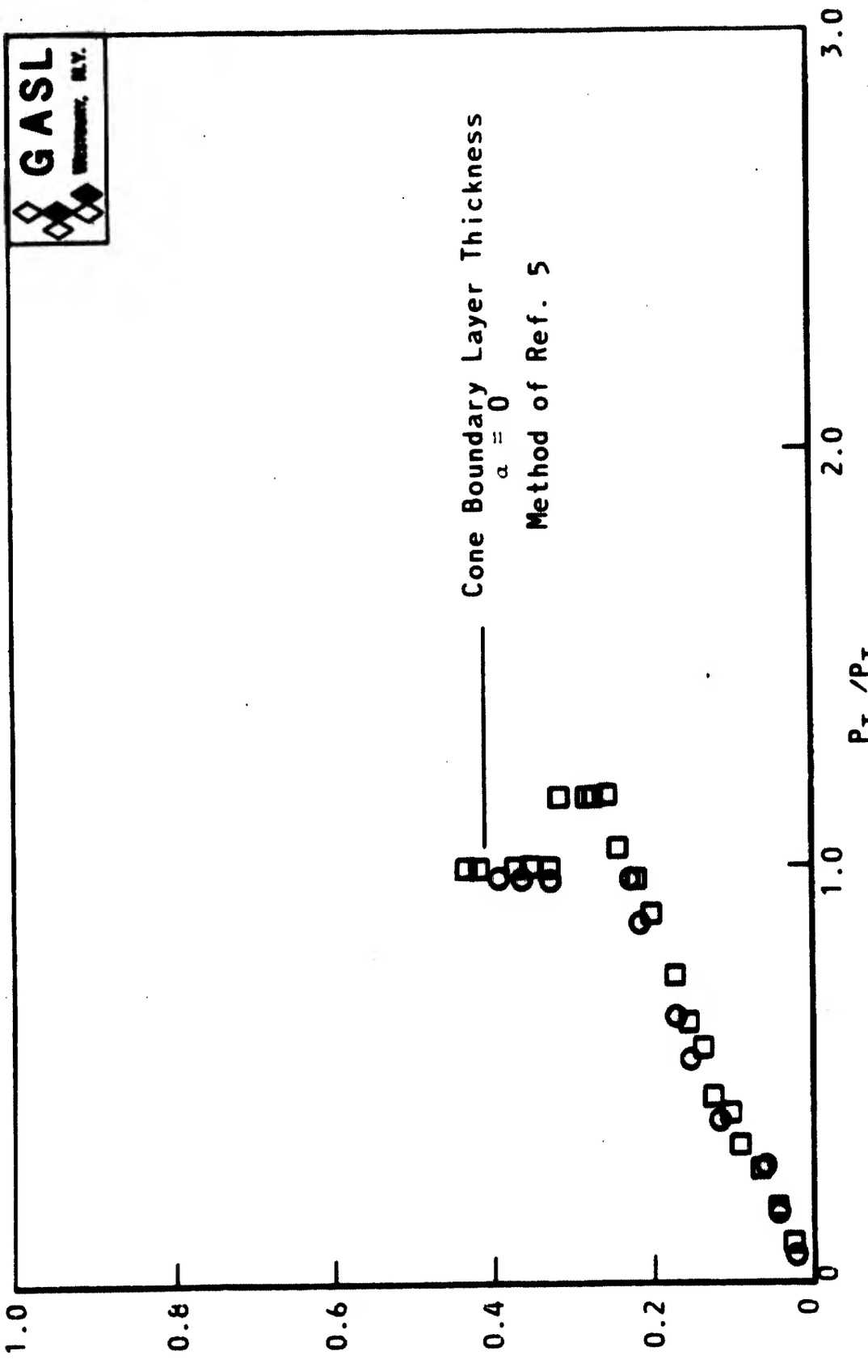

FIGURE 10: BOUNDARY LAYER PITOT PROFILE AT CONE SHOULDER LEEWARD SIDE

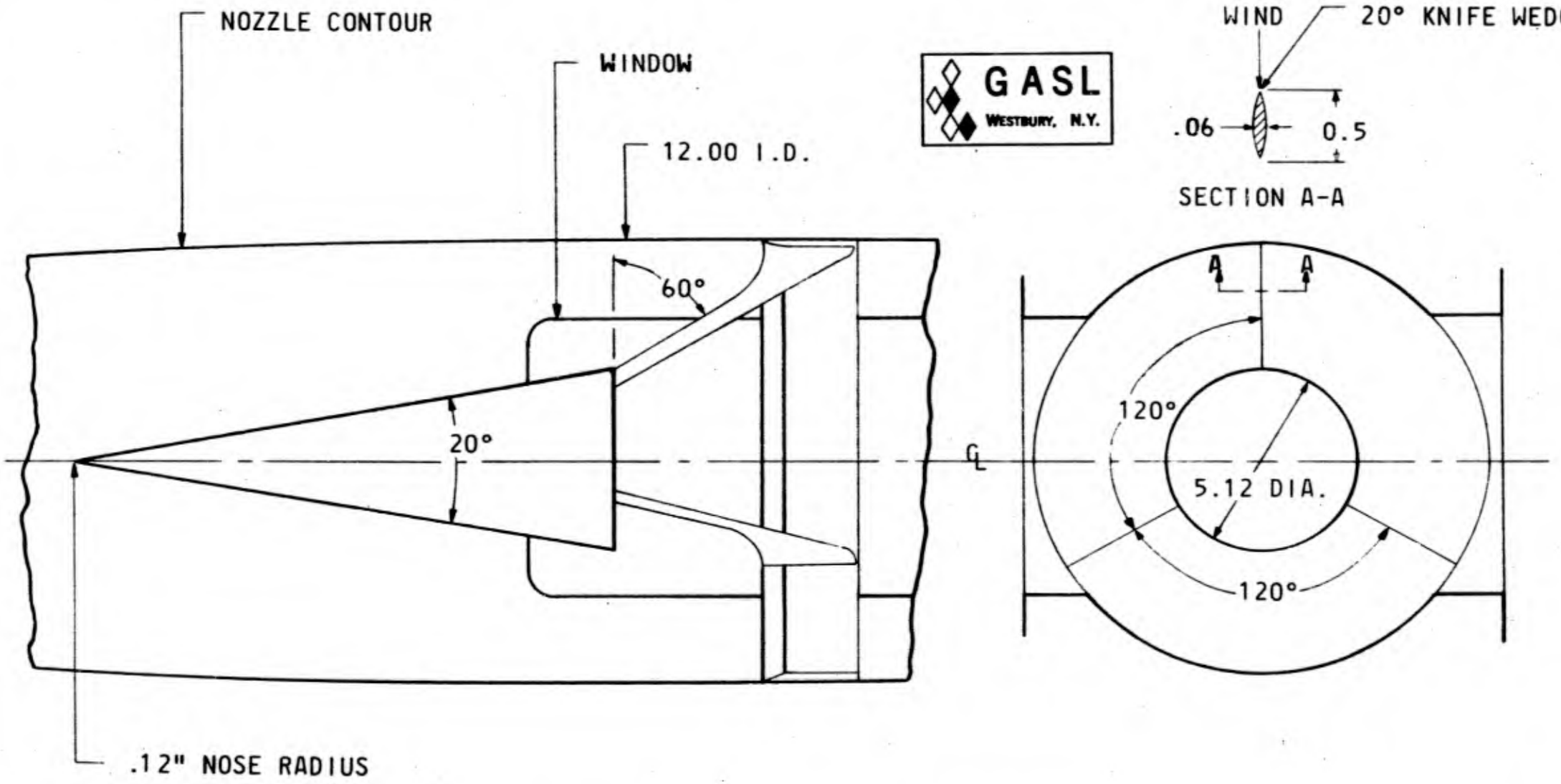

FIGURE 11: MODEL SUPPORT - CONFIGURATION 'C'

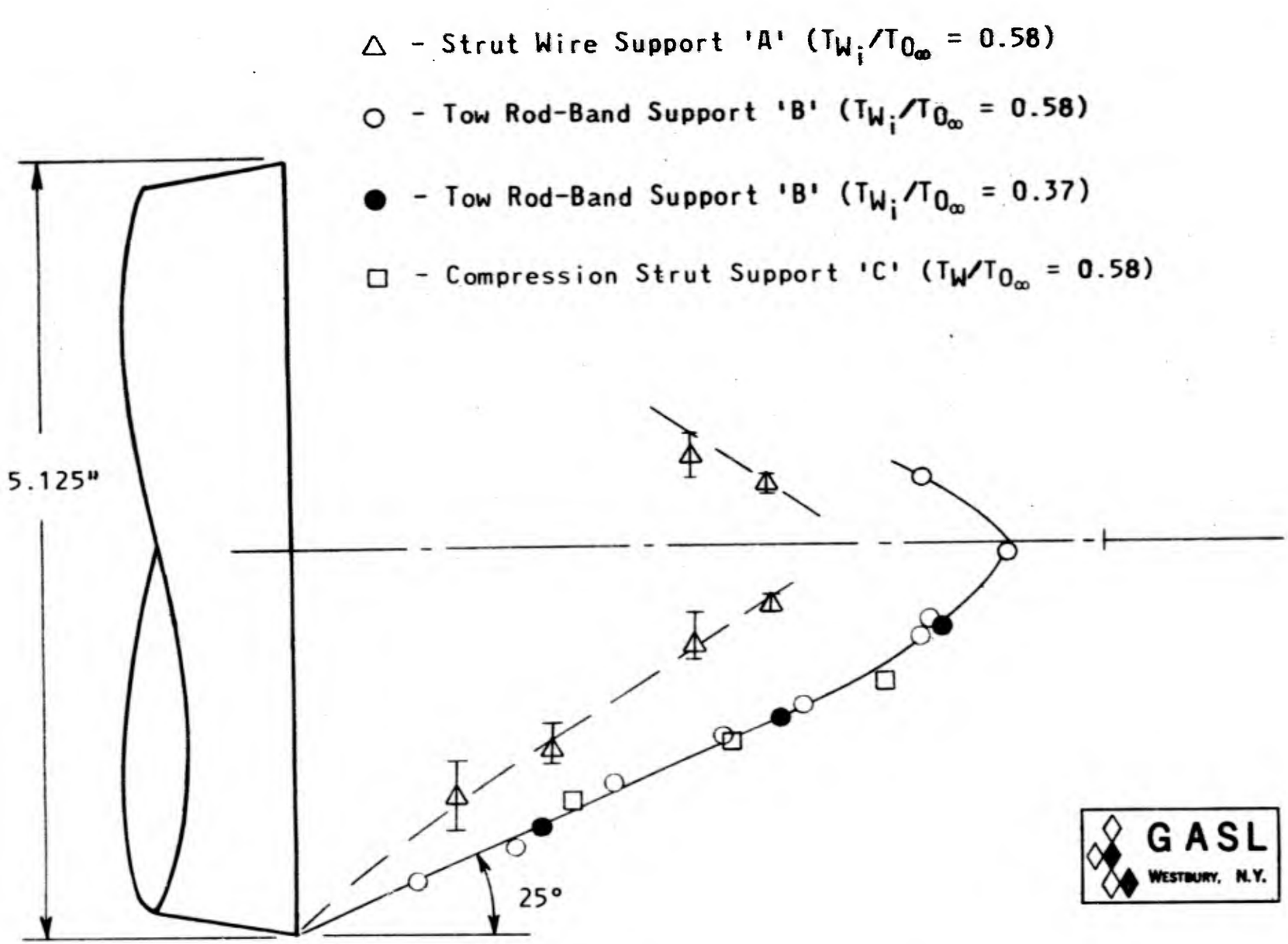

FIGURE 12: u = 0 LINE

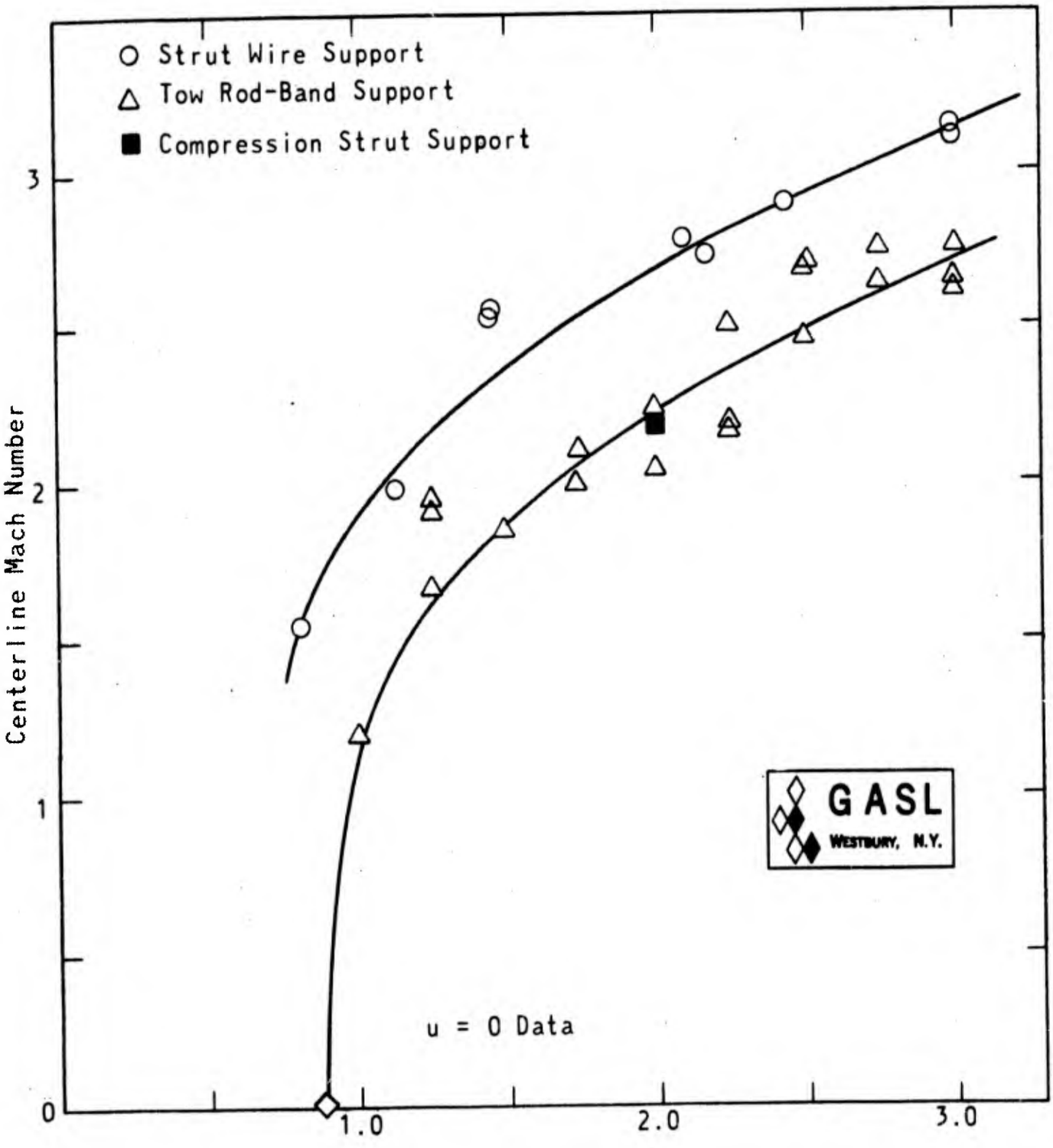

FIGURE 13: CENTERLINE MACH NUMBER DISTRIBUTION

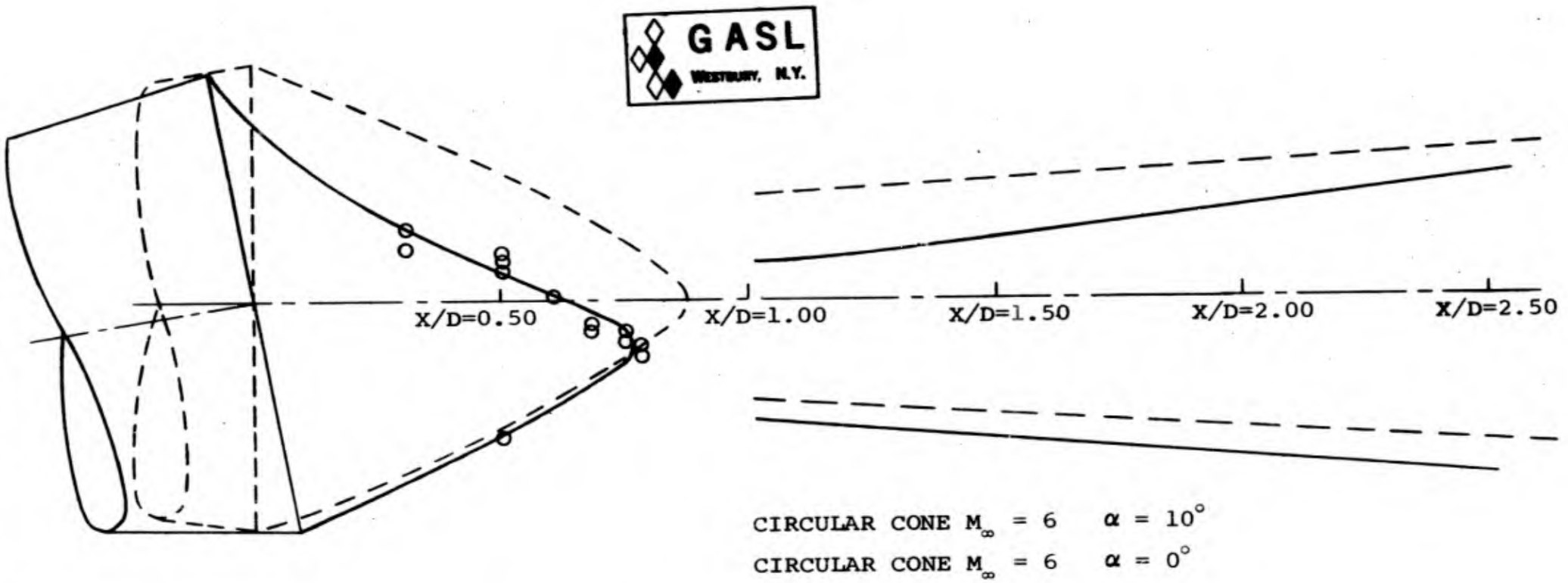

FIG. 14: "u = 0" LINE AND TRAILING SHOCK SHAPE

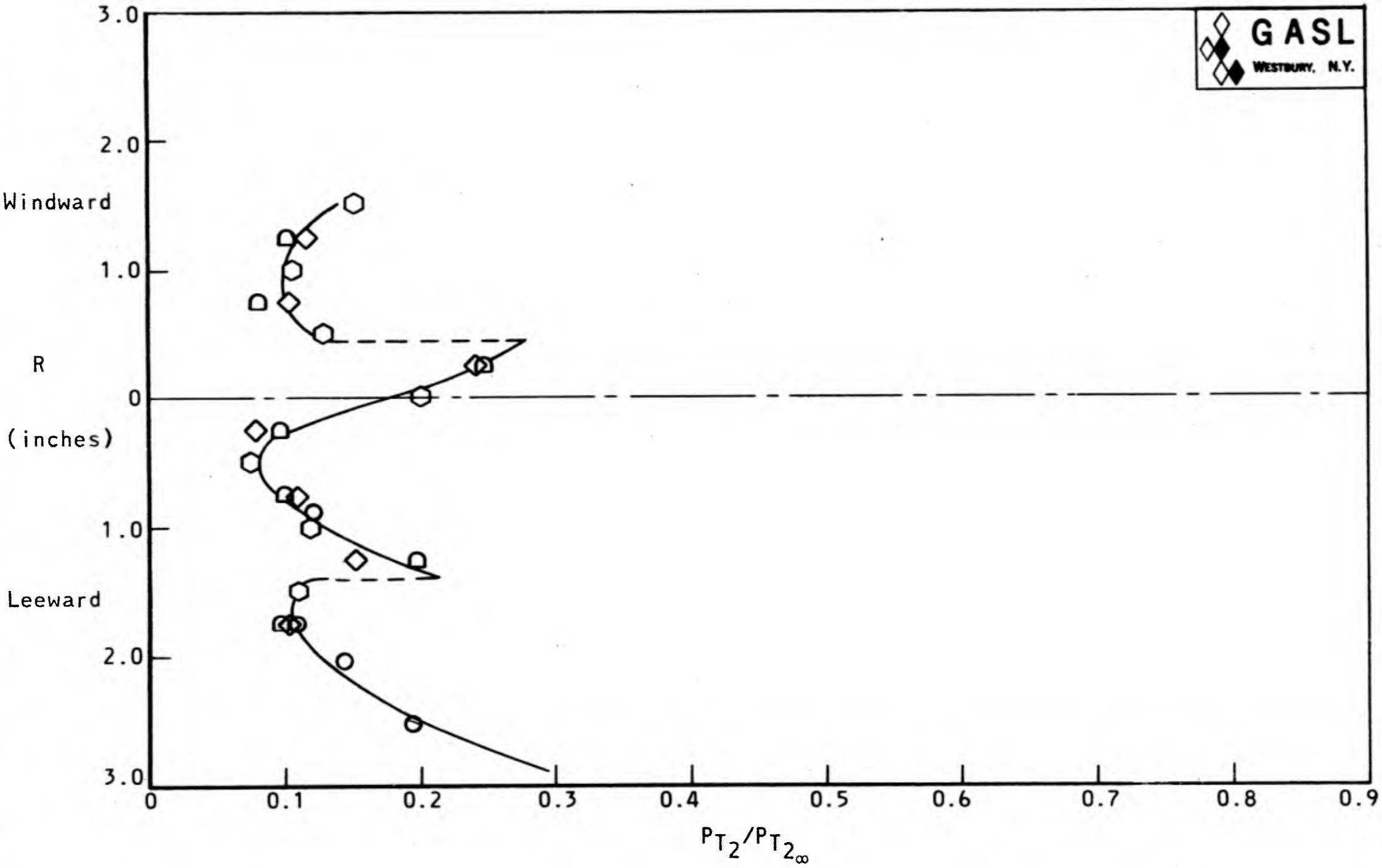

FIGURE 15A: RADIAL PITOT PRESSURE PROFILE X/D = 1.00

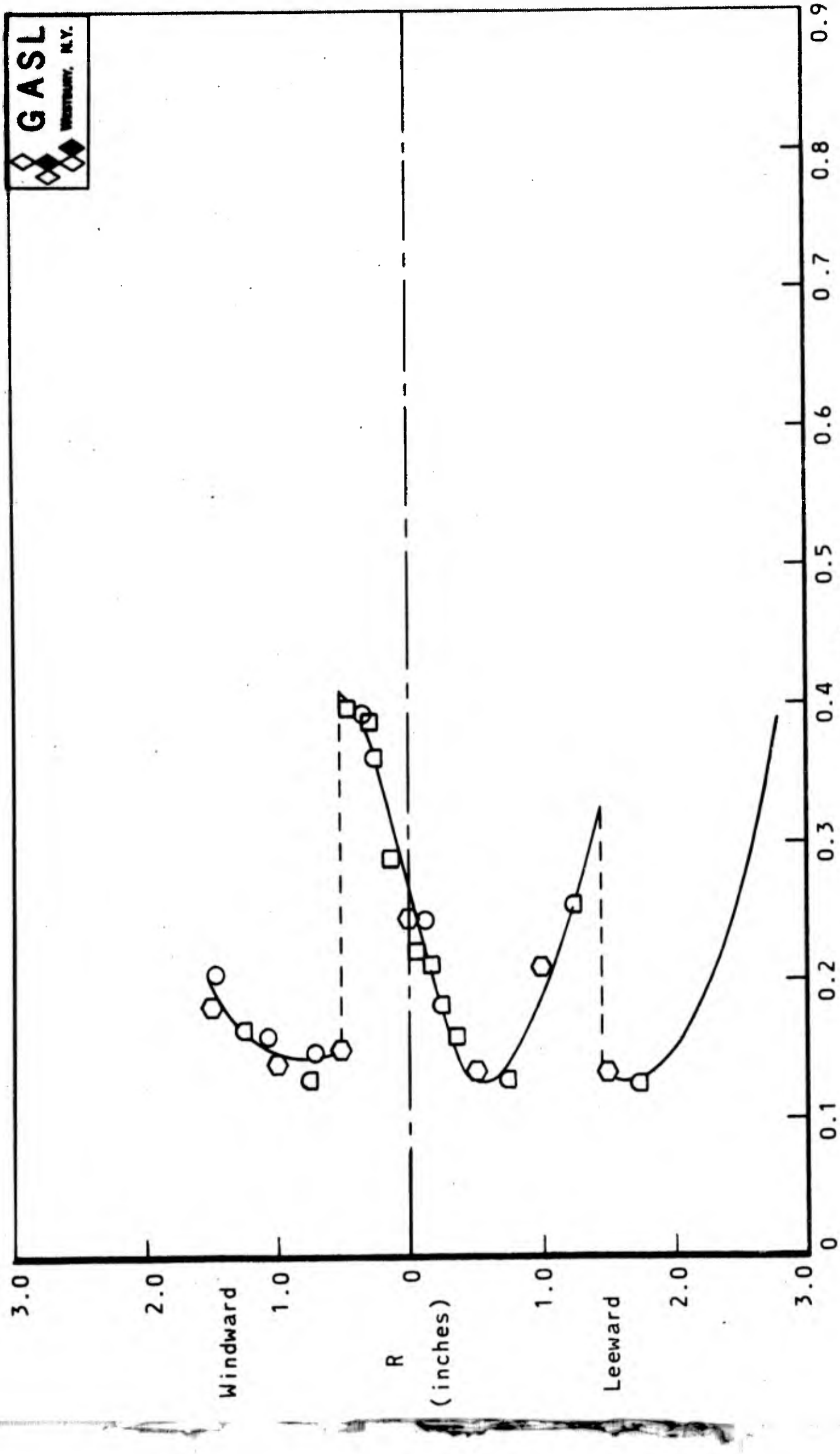

FIGURE 15B: RADIAL PITOT PRESSURE PROFILE X/D = 1.25

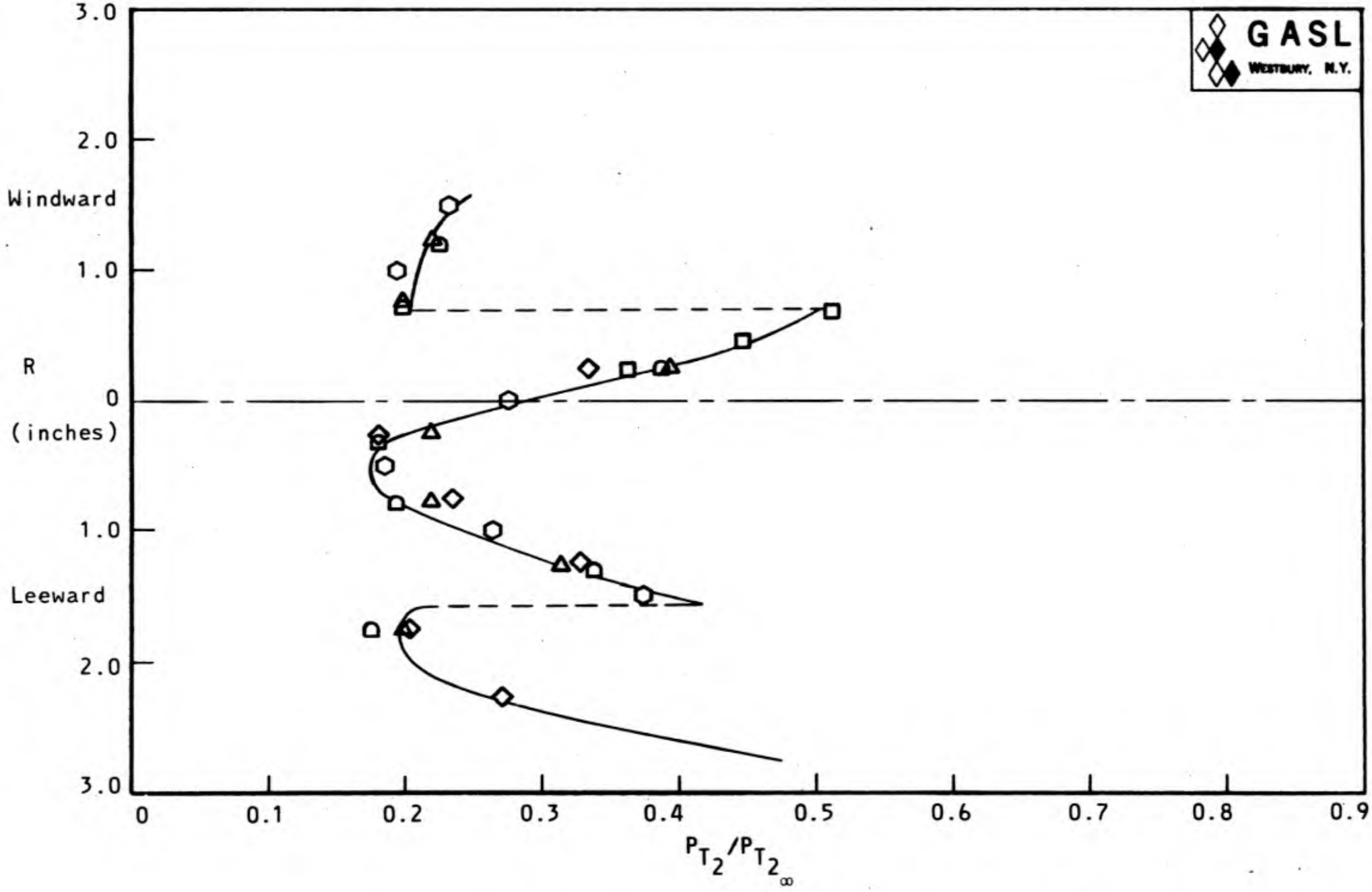

FIGURE 15C: RADIAL PITOT PRESSURE PROFILE X/D = 1.50

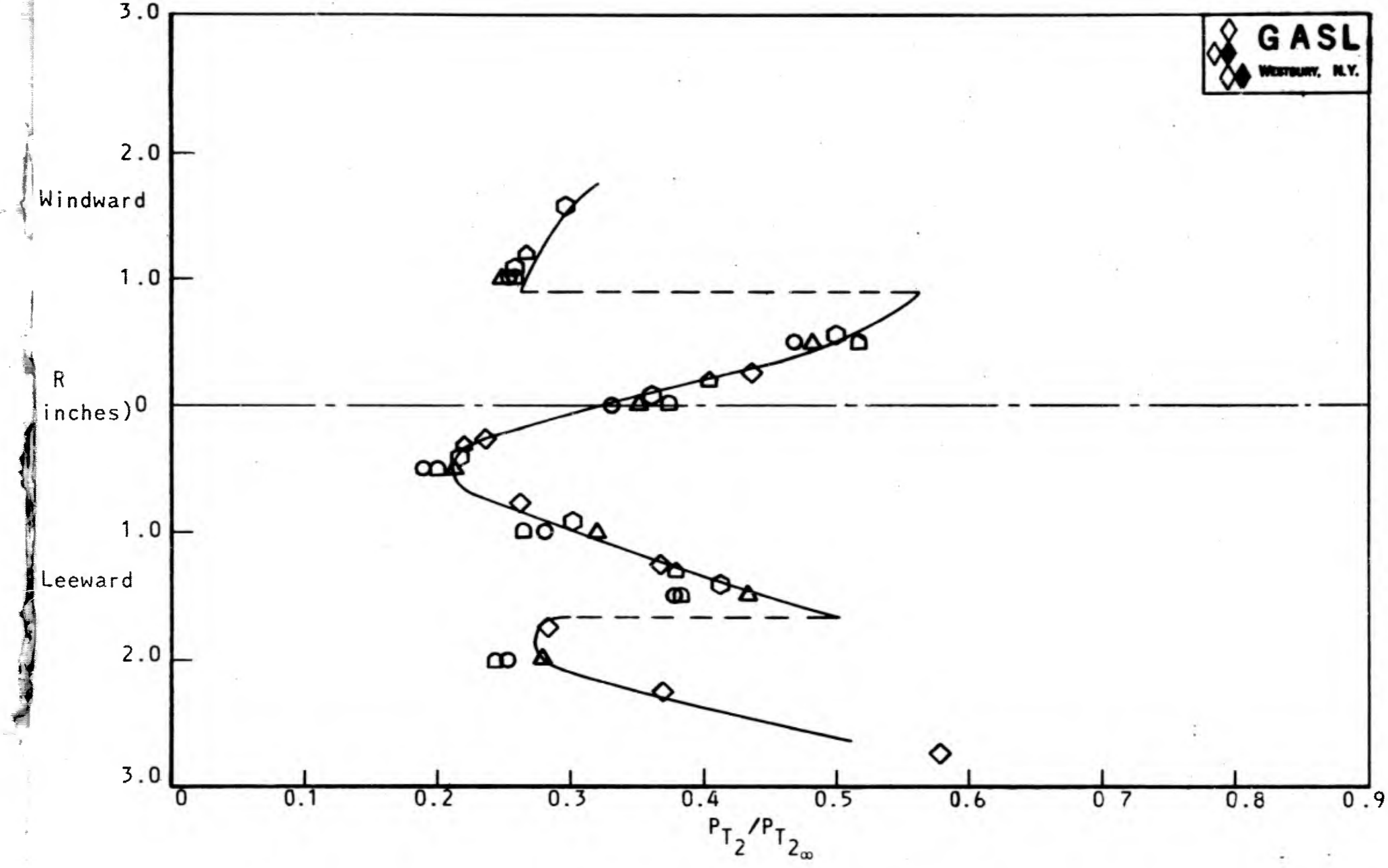

FIGURE 15D: RADIAL PITOT PRESSURE PROFILE X/D = 1.75

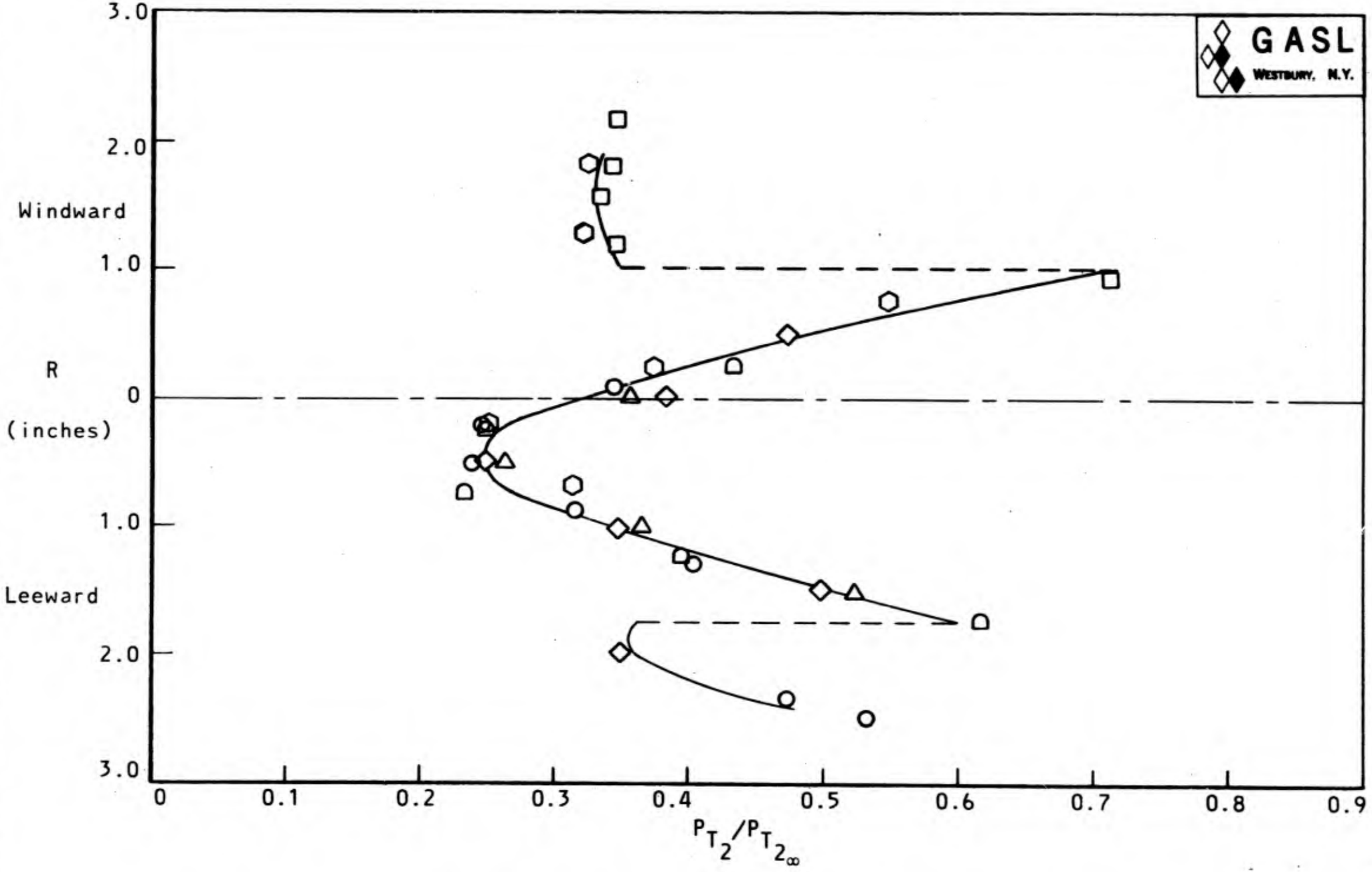

FIGURE 15E: RADIAL PITOT PRESSURE PROFILE X/D = 2.00

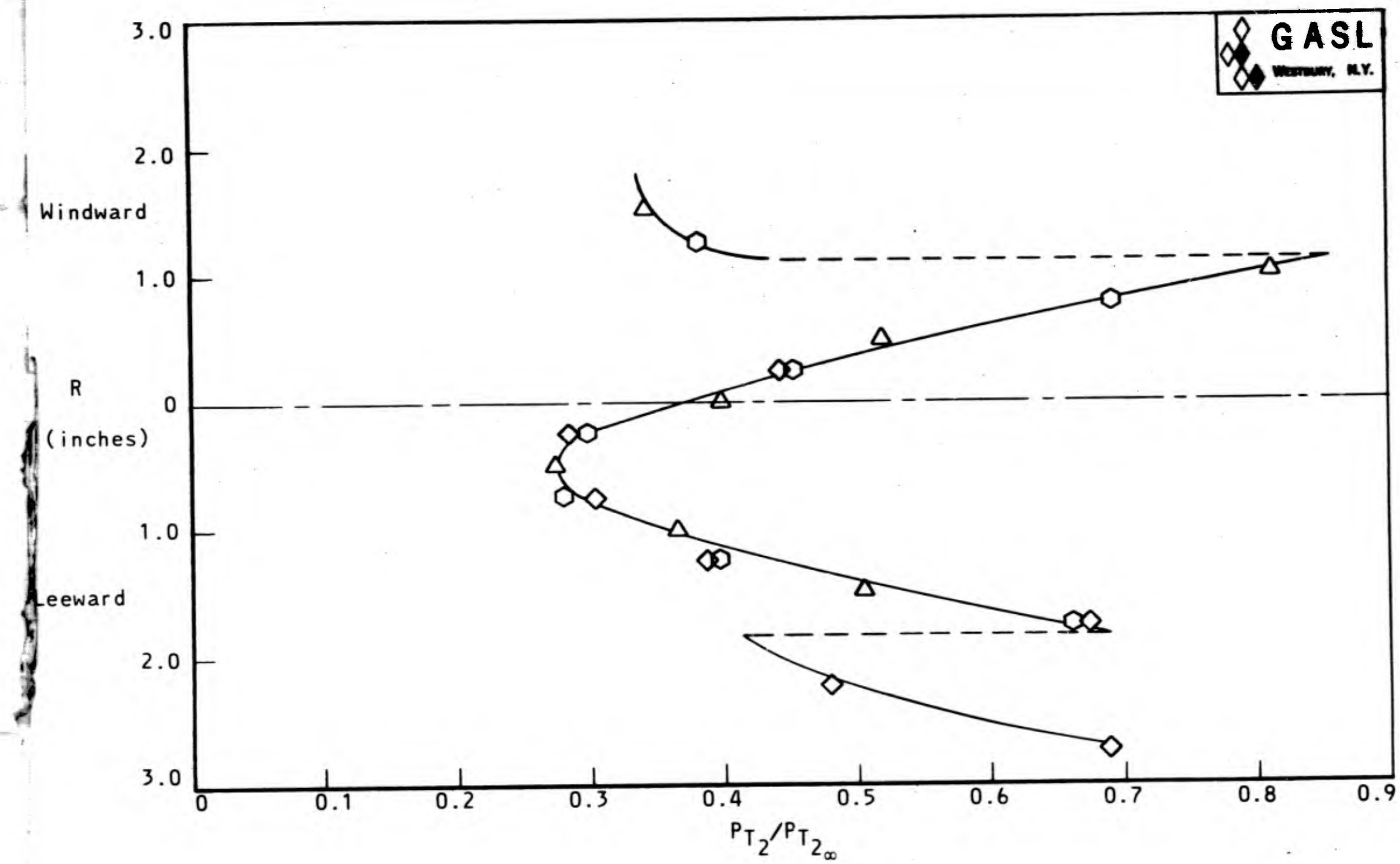

FIGURE 15F: RADIAL PITOT PRESSURE PROFILE X/D = 2.25

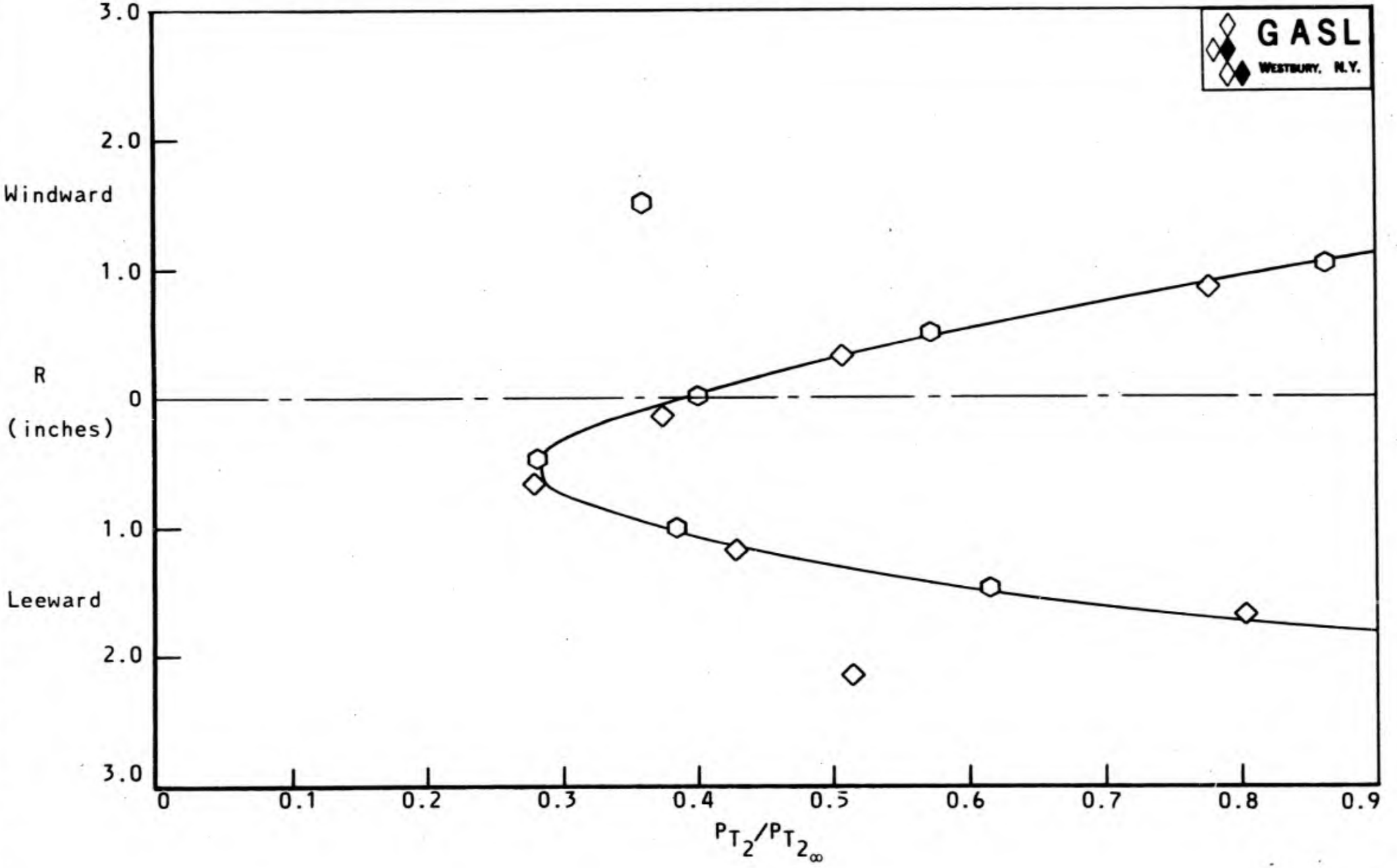

FIGURE 15G: RADIAL PITOT PRESSURE PROFILE X/D = 2.50

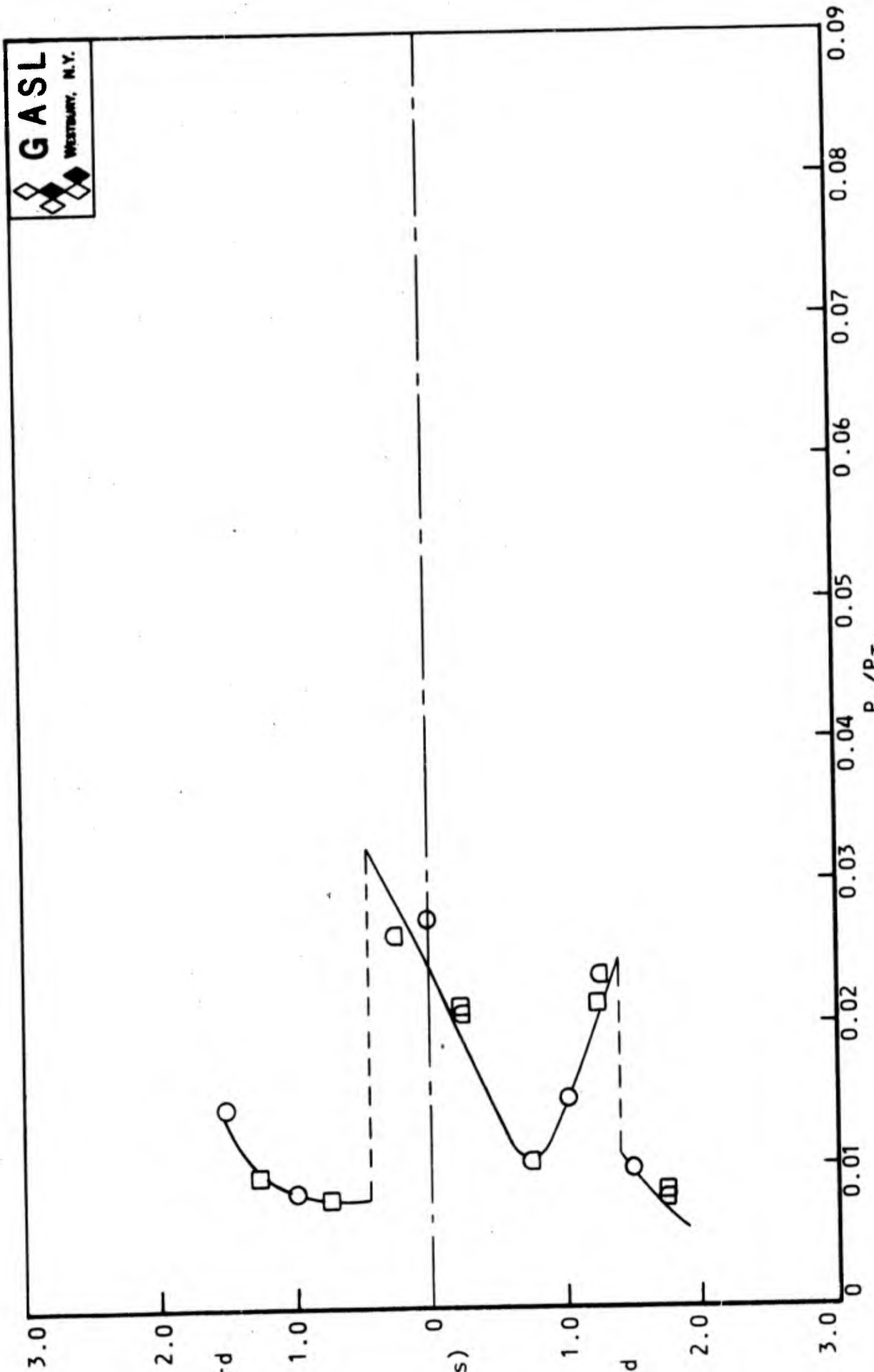

FIGURE 16A: RADIAL CONE PROBE PRESSURE PROFILE X/D = 1.00

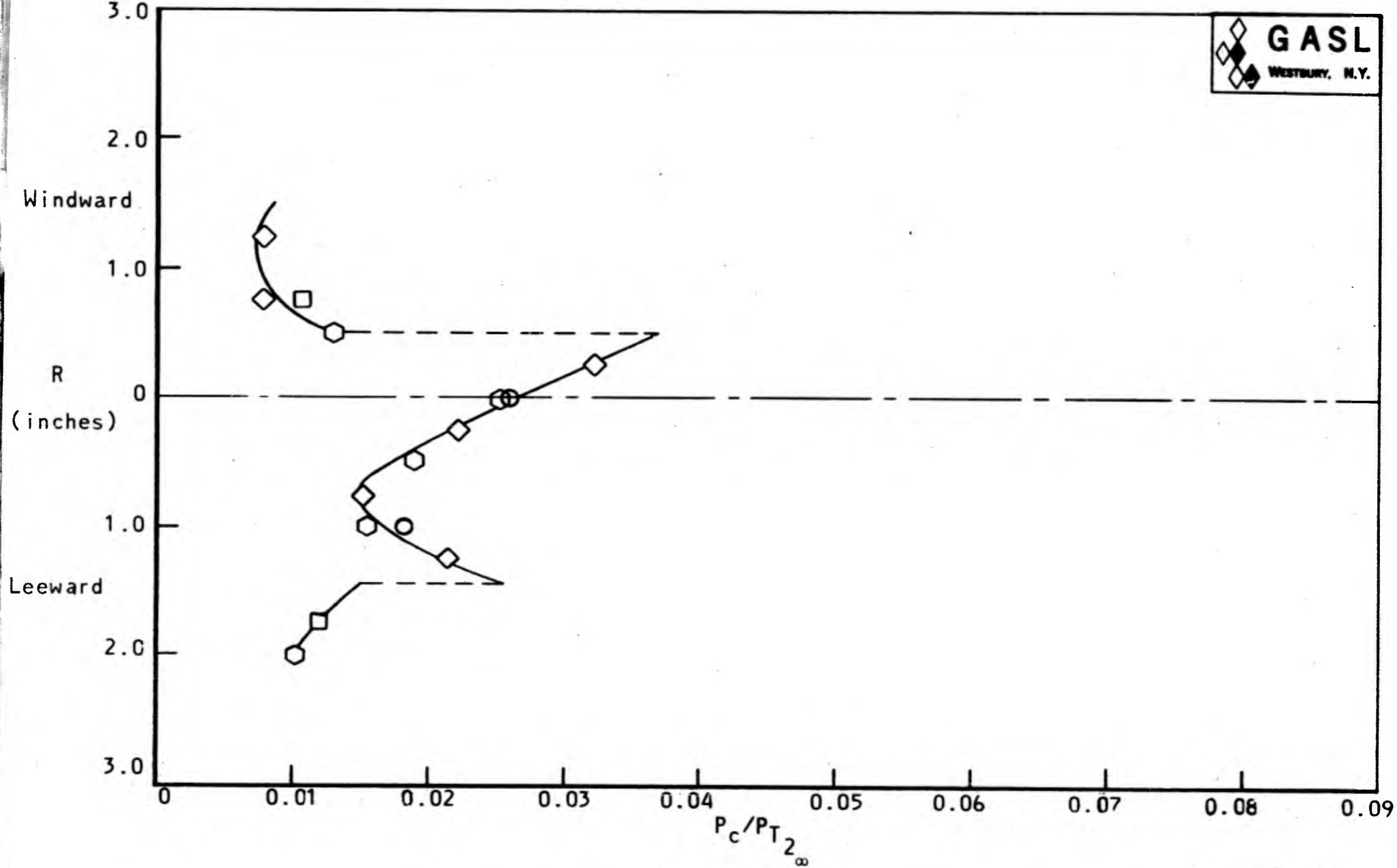

FIGURE 16B: RADIAL CONE PROBE PRESSURE PROFILE X/D = 1.25

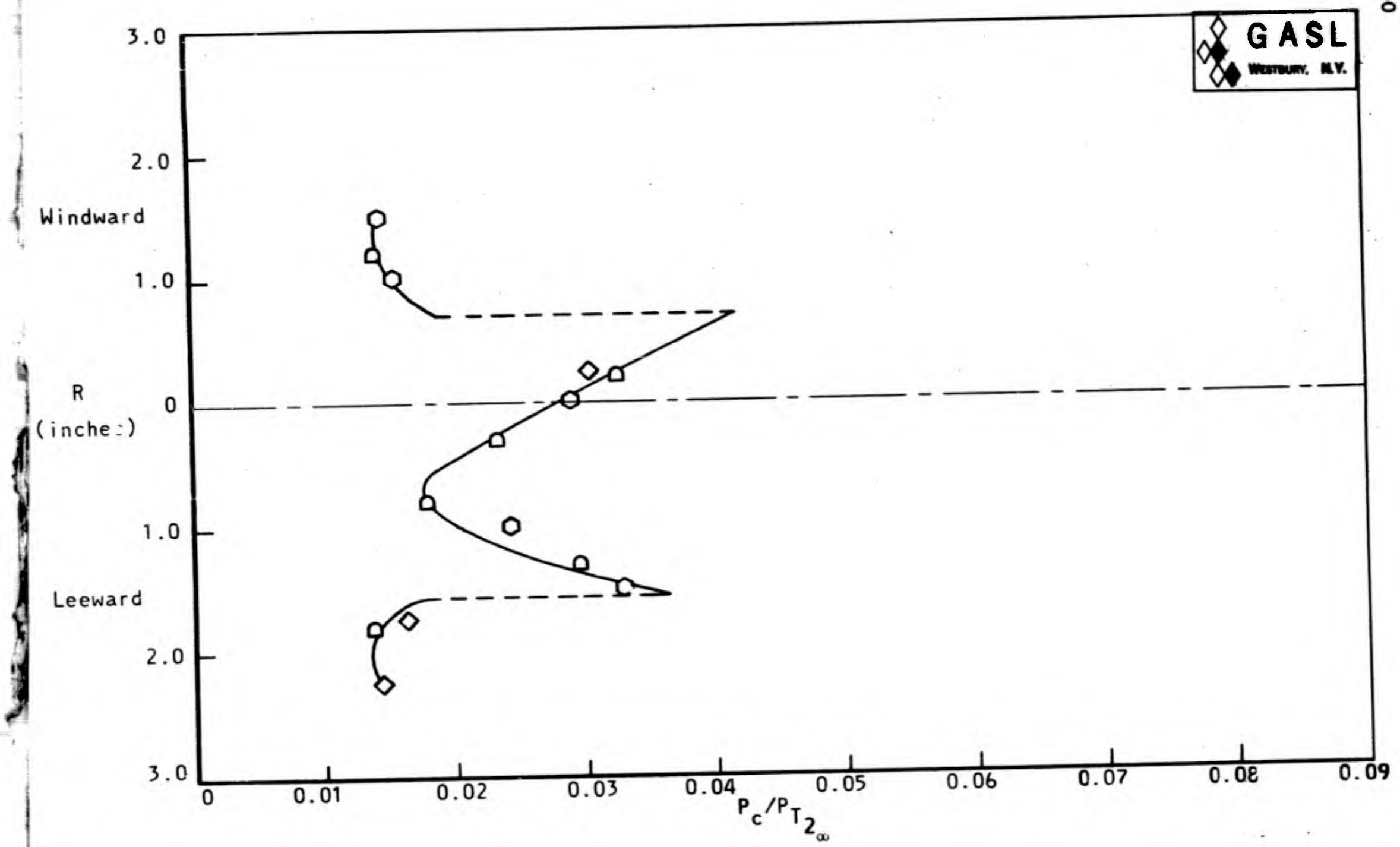

FIGURE 16C: RADIAL CONE PROBE PRDSSURE PROFILE X/D = 1.50

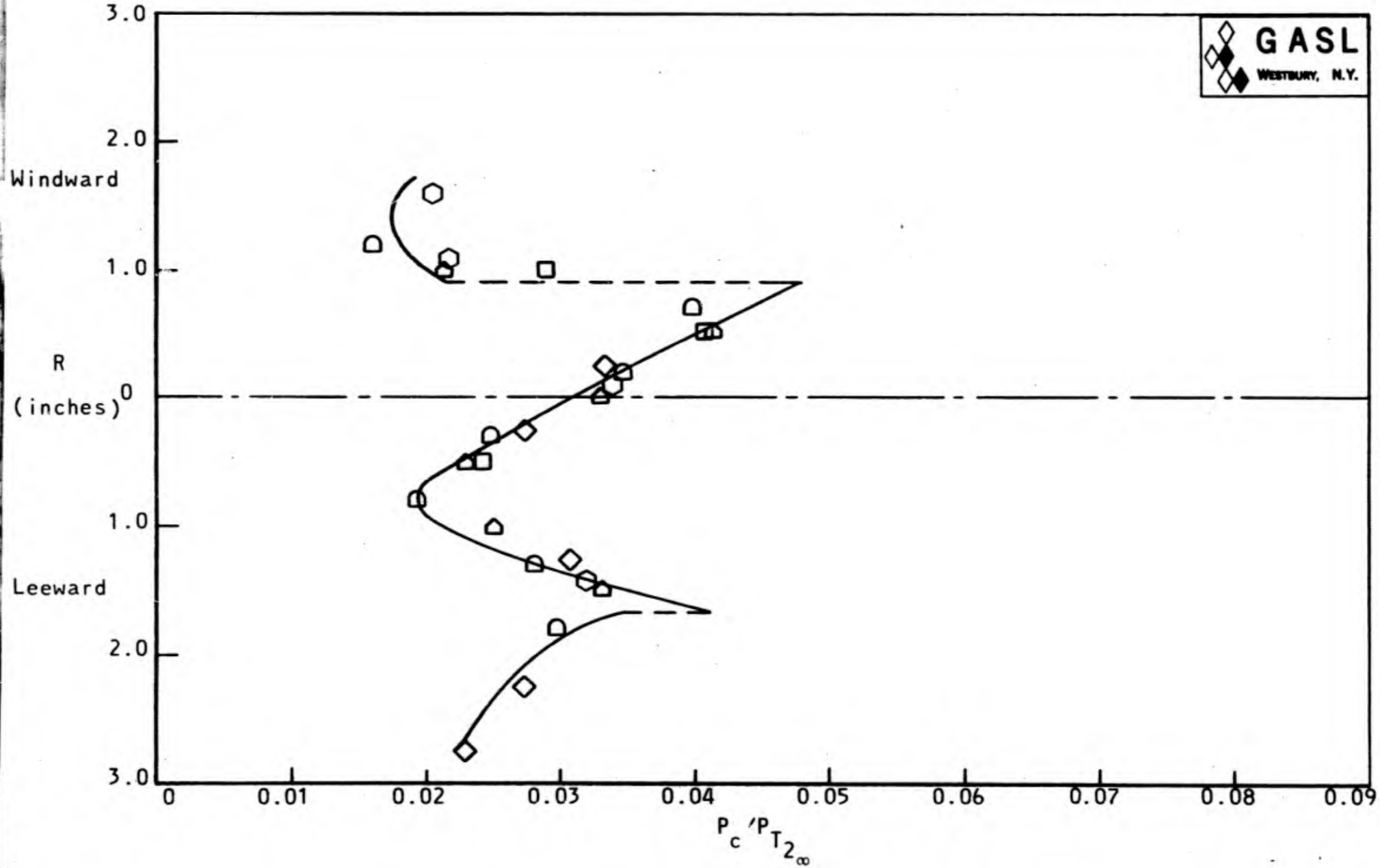

FIGURE 16D: RADIAL CONE PROBE PRESSURE PROFILE X/D = 1.75

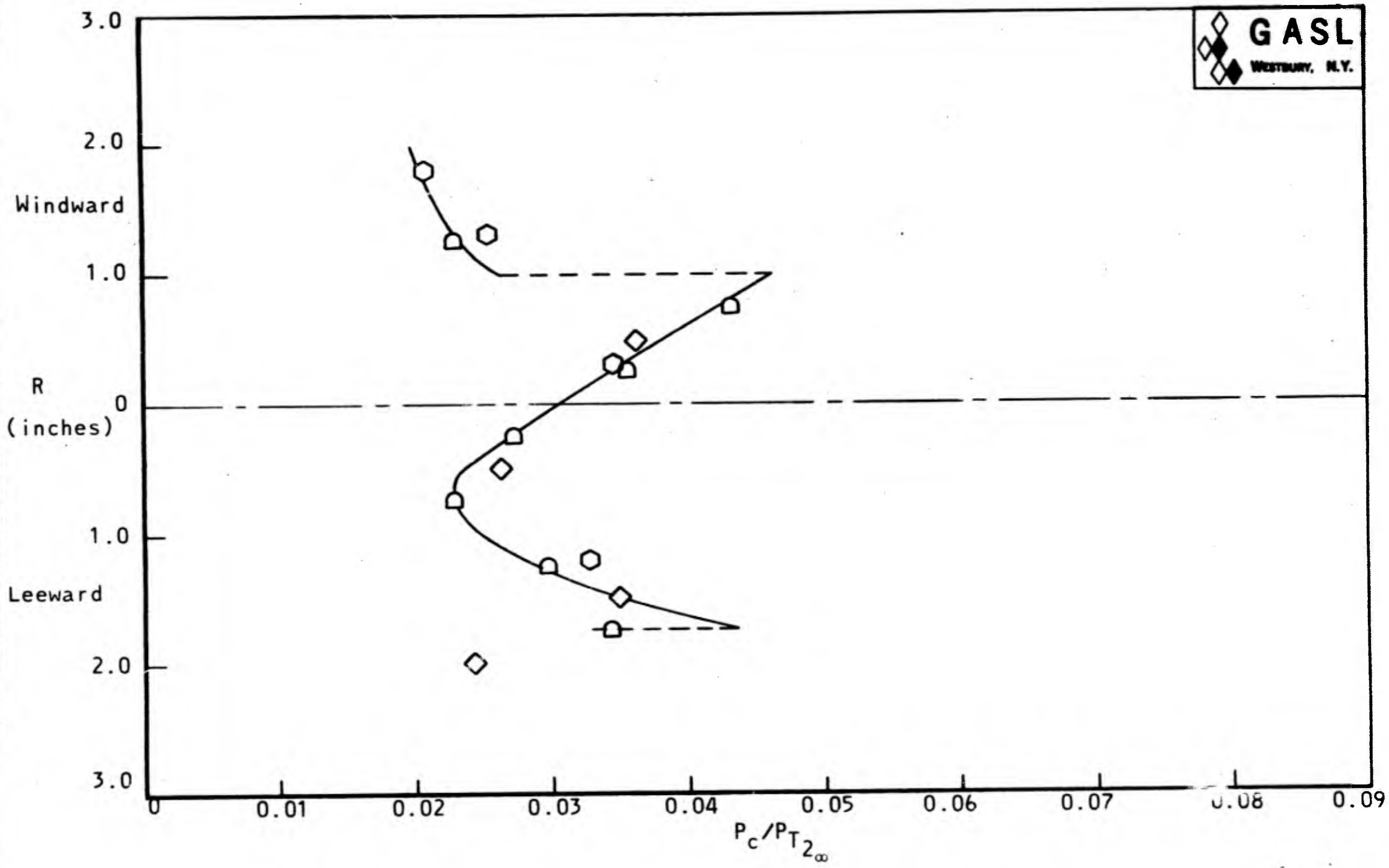

FIGURE 16E: RADIAL CONE PROBE PRESSURE PROFILE X/D = 2.00

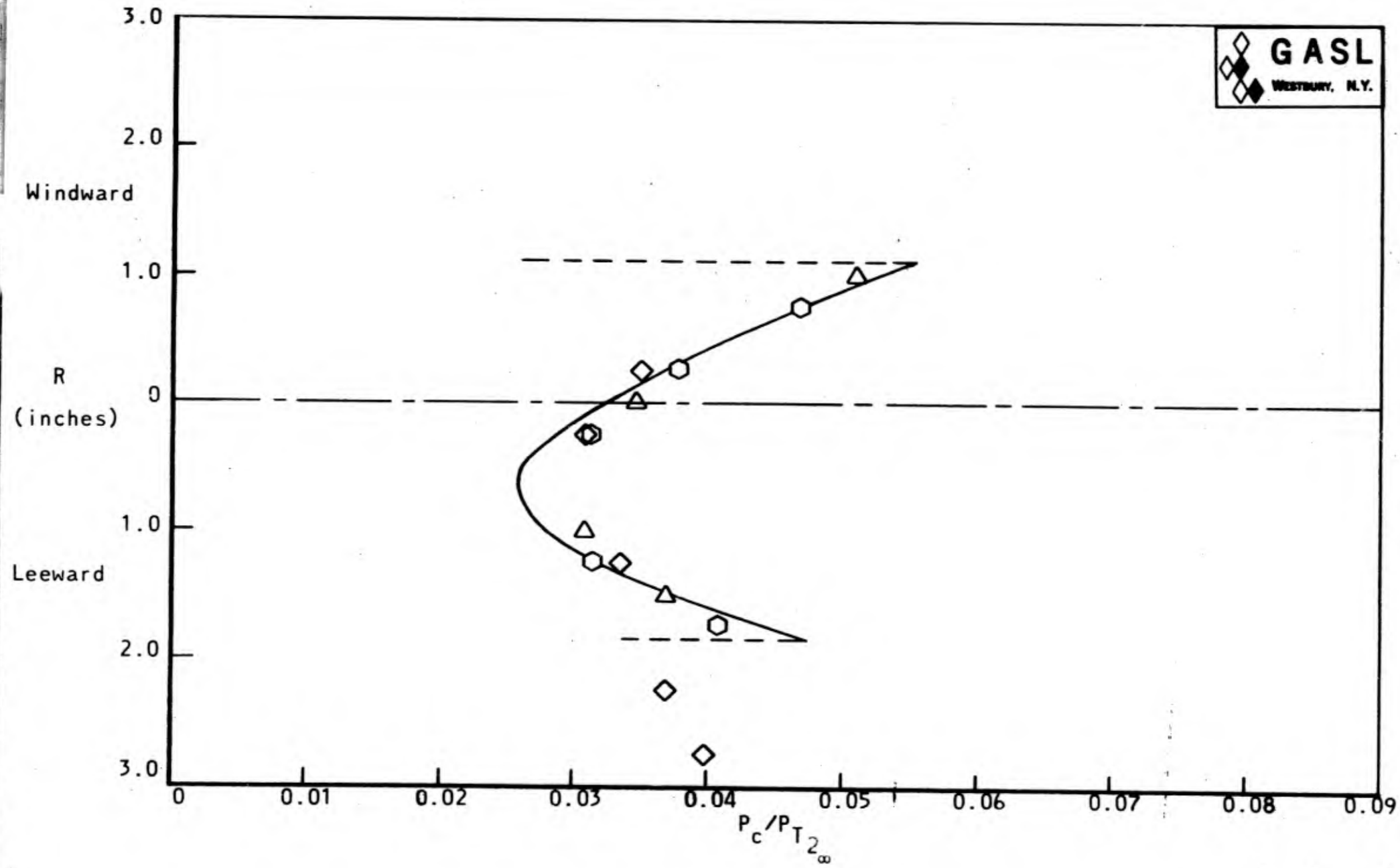

FIGURE 16F: RADIAL CONE PROBE PRESSURE PROFILE X/D = 2.25

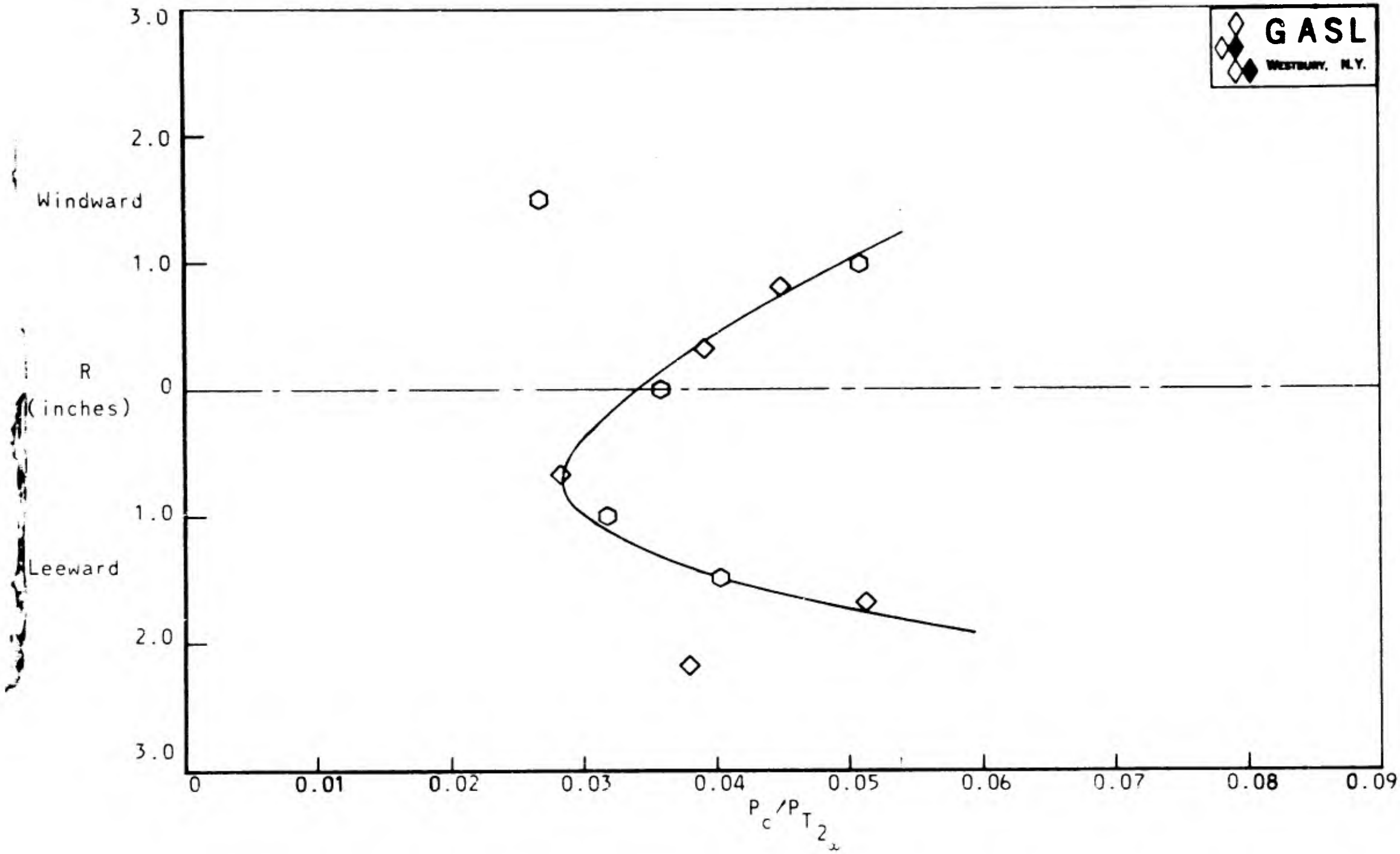

FIGURE 16G RADIAL CONE PROBE PRESSURE PROFILE X/D = 2.50

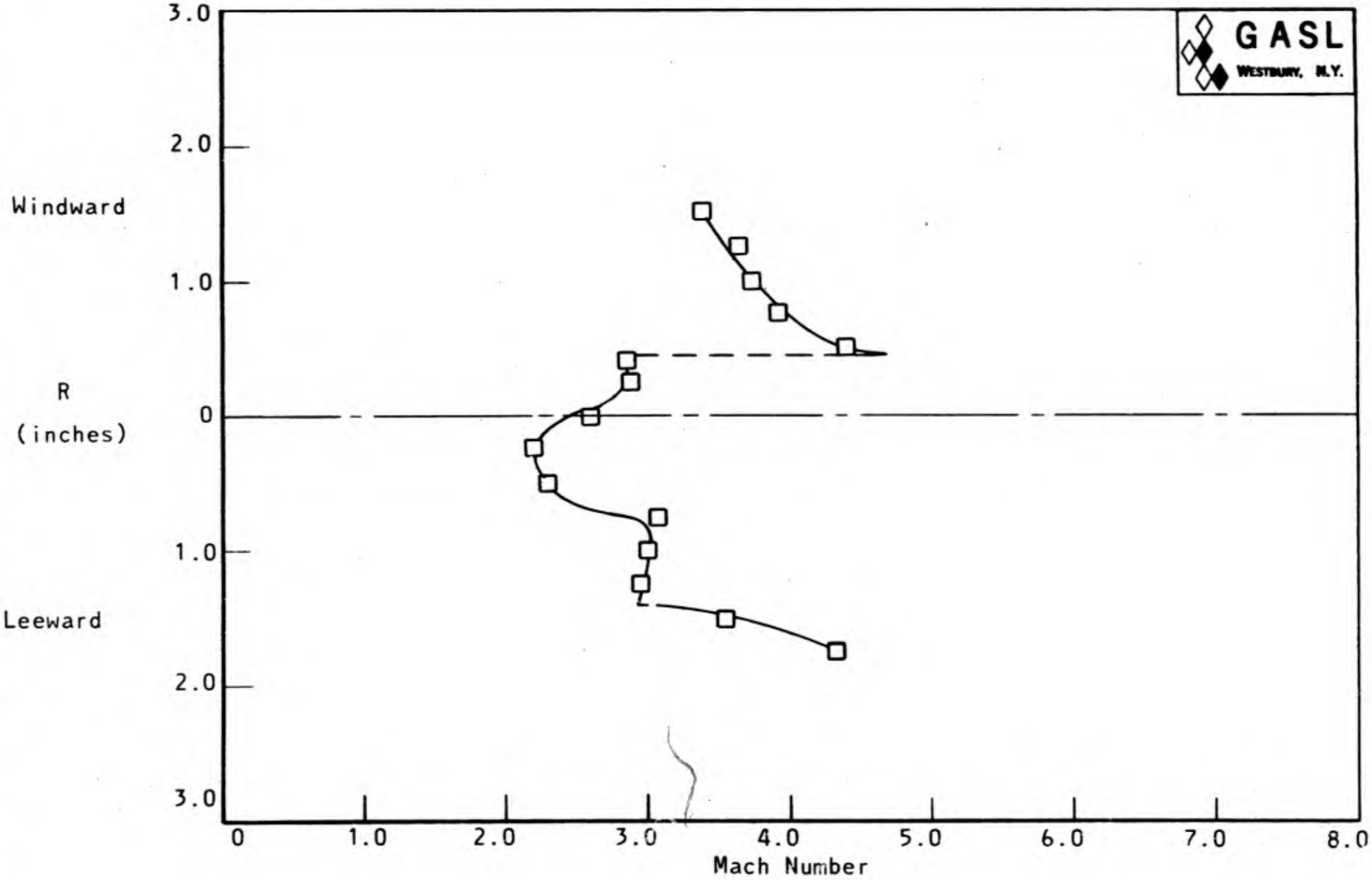

FIGURE 17A: MACH NUMBER PROFILE X/D = 1.00

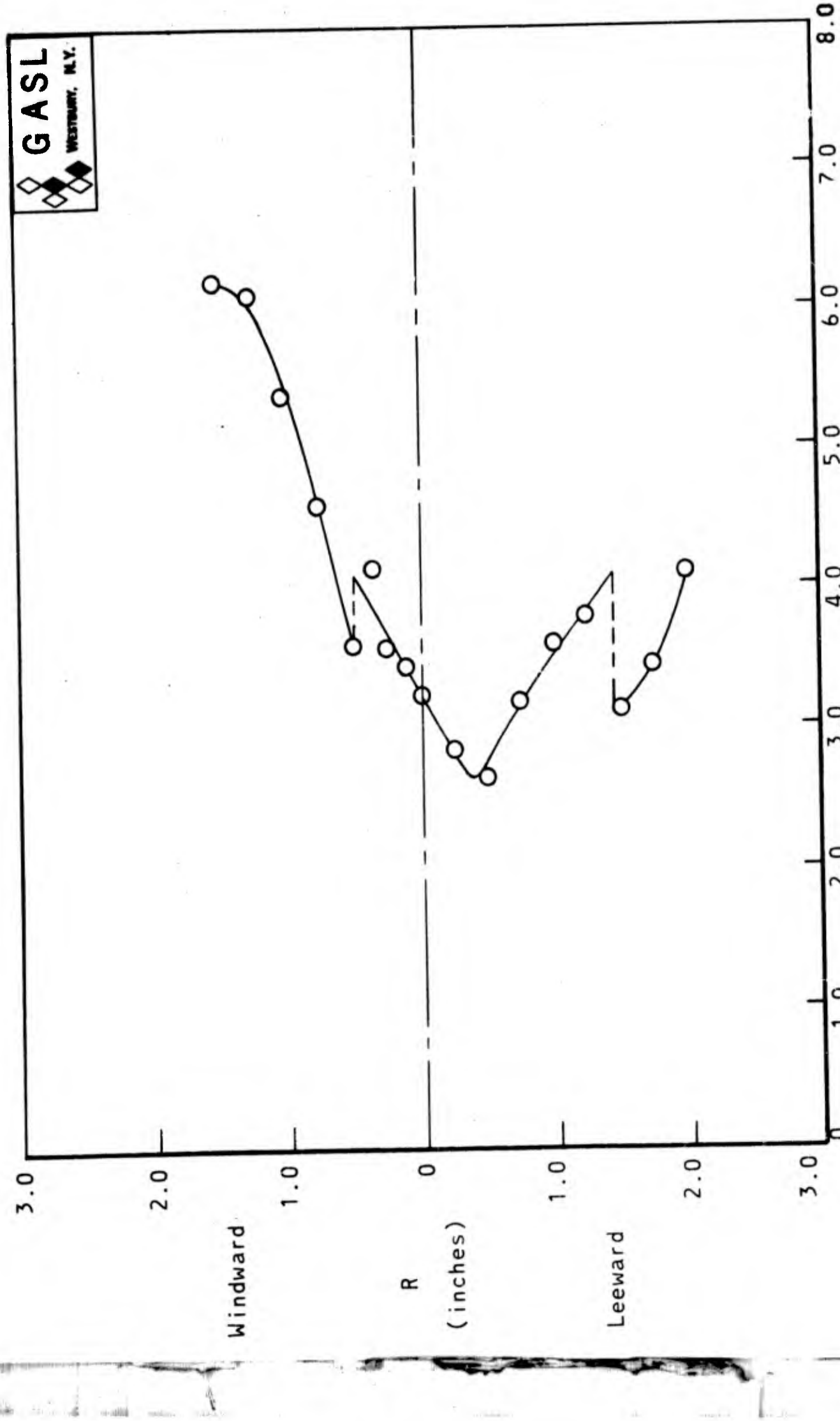

FIGURE 17B: MACH NUMBER PROFILE X/D = 1.25

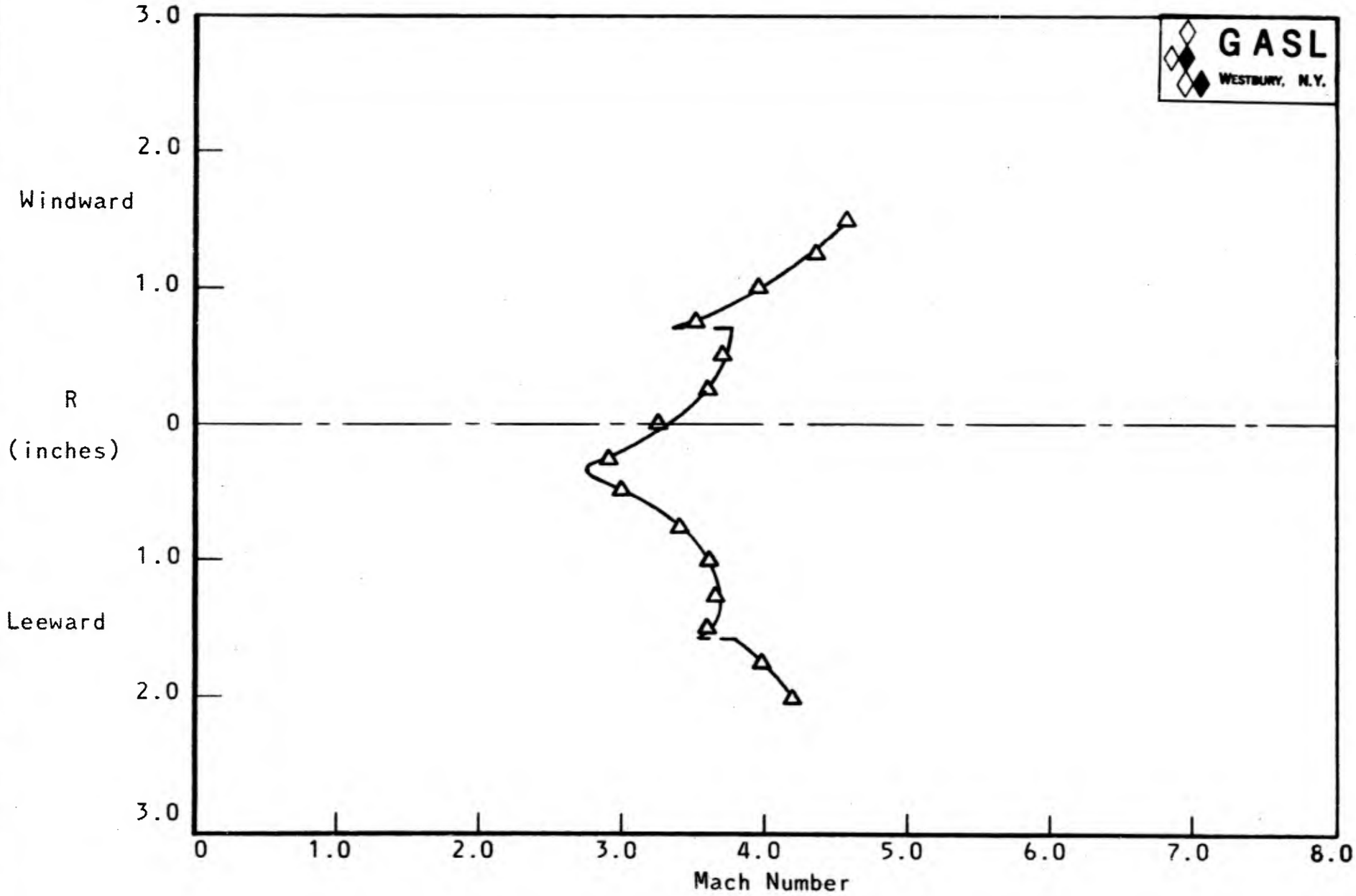

FIGURE 17C: MACH NUMBER PROFILE X/D = 1.50

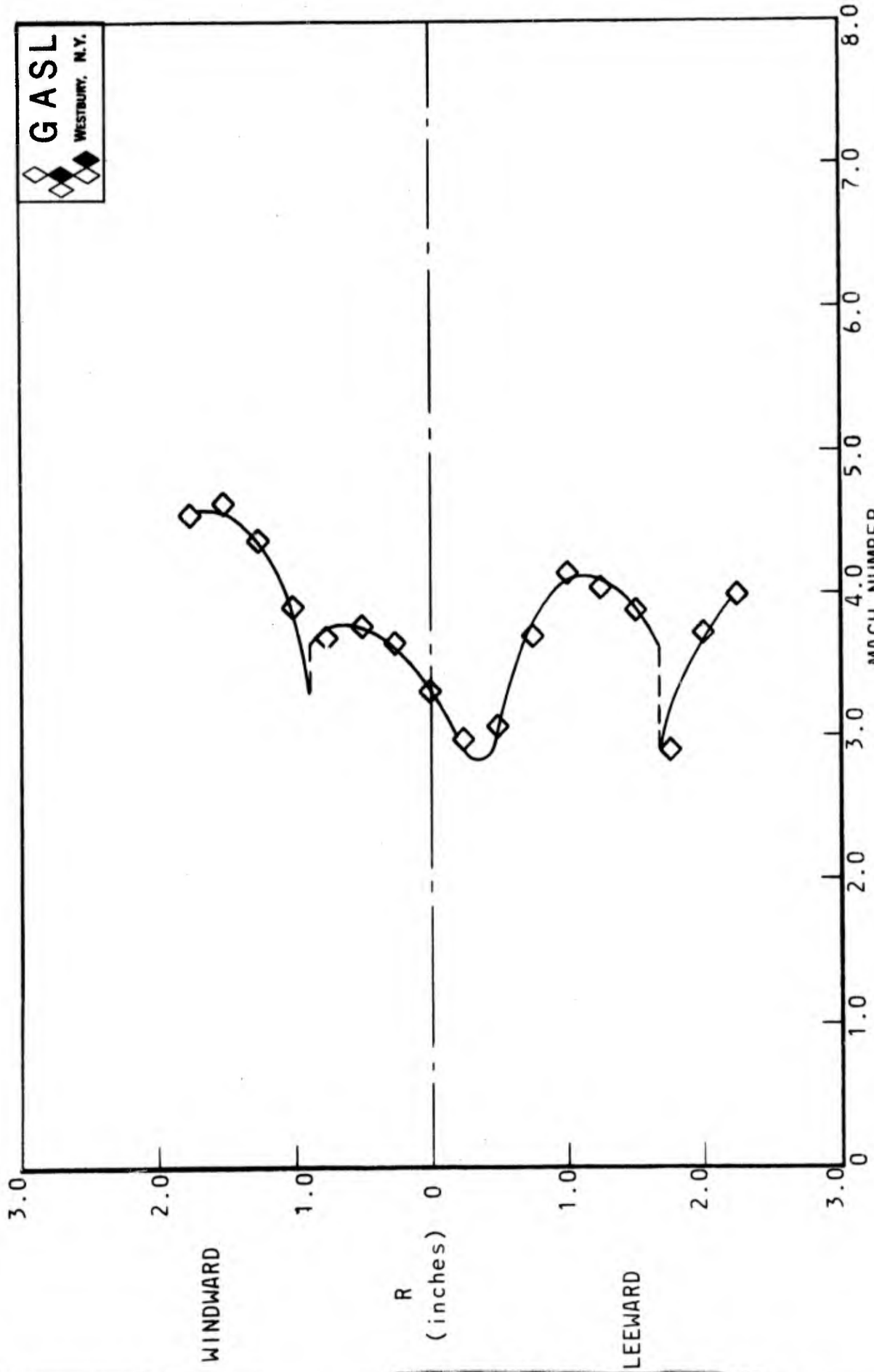

FIGURE 17D: RADIAL MACH NUMBER PROFILE X/D = 1.75

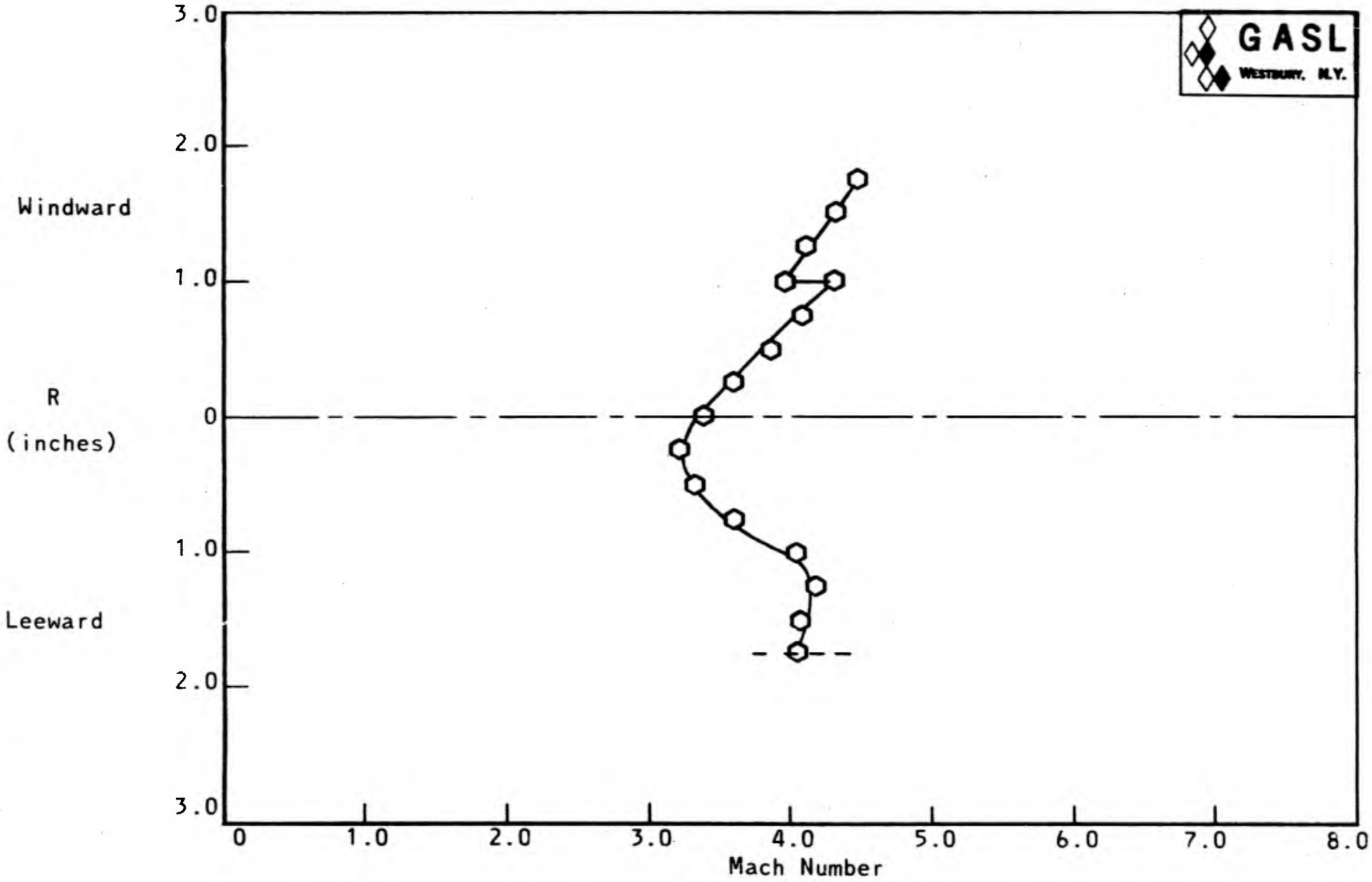

FIGURE 17E: MACH NUMBER PROFILE X/D = 2.00

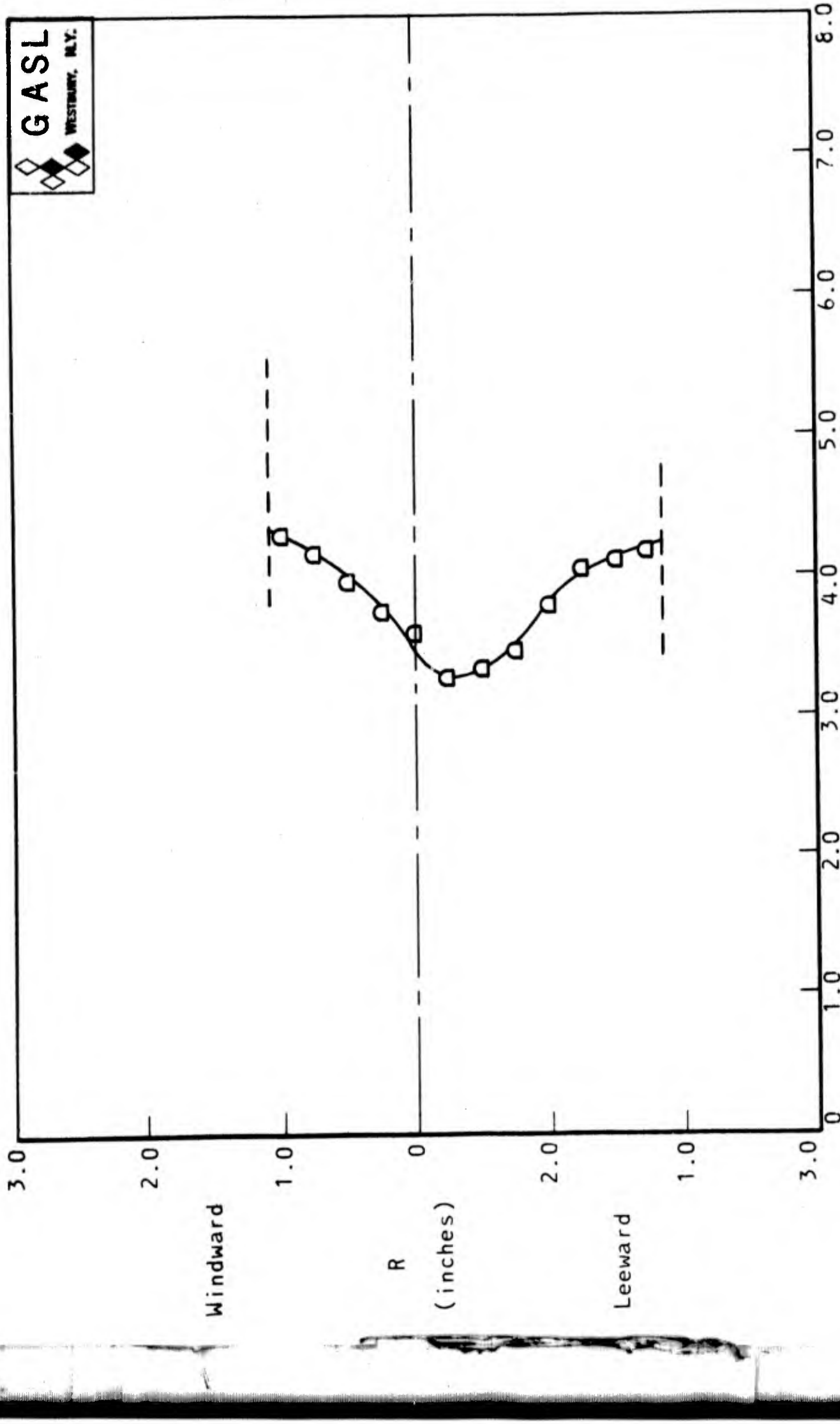

FIGURE 17F: MACH NUMBER PROFILE X/D = 2.25

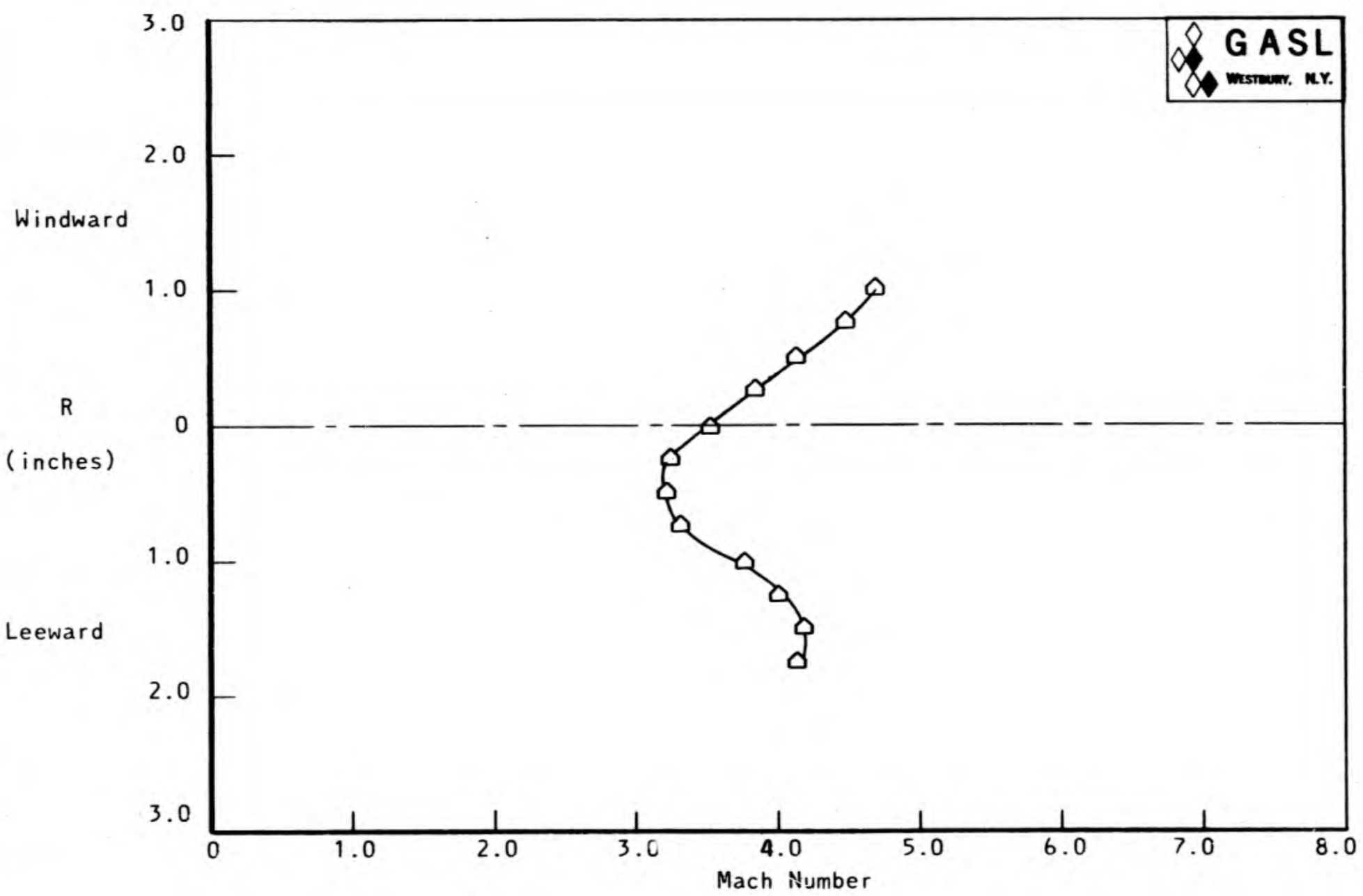

FIGURE 17G: MACH NUMBER PROFILE X/D = 2.50

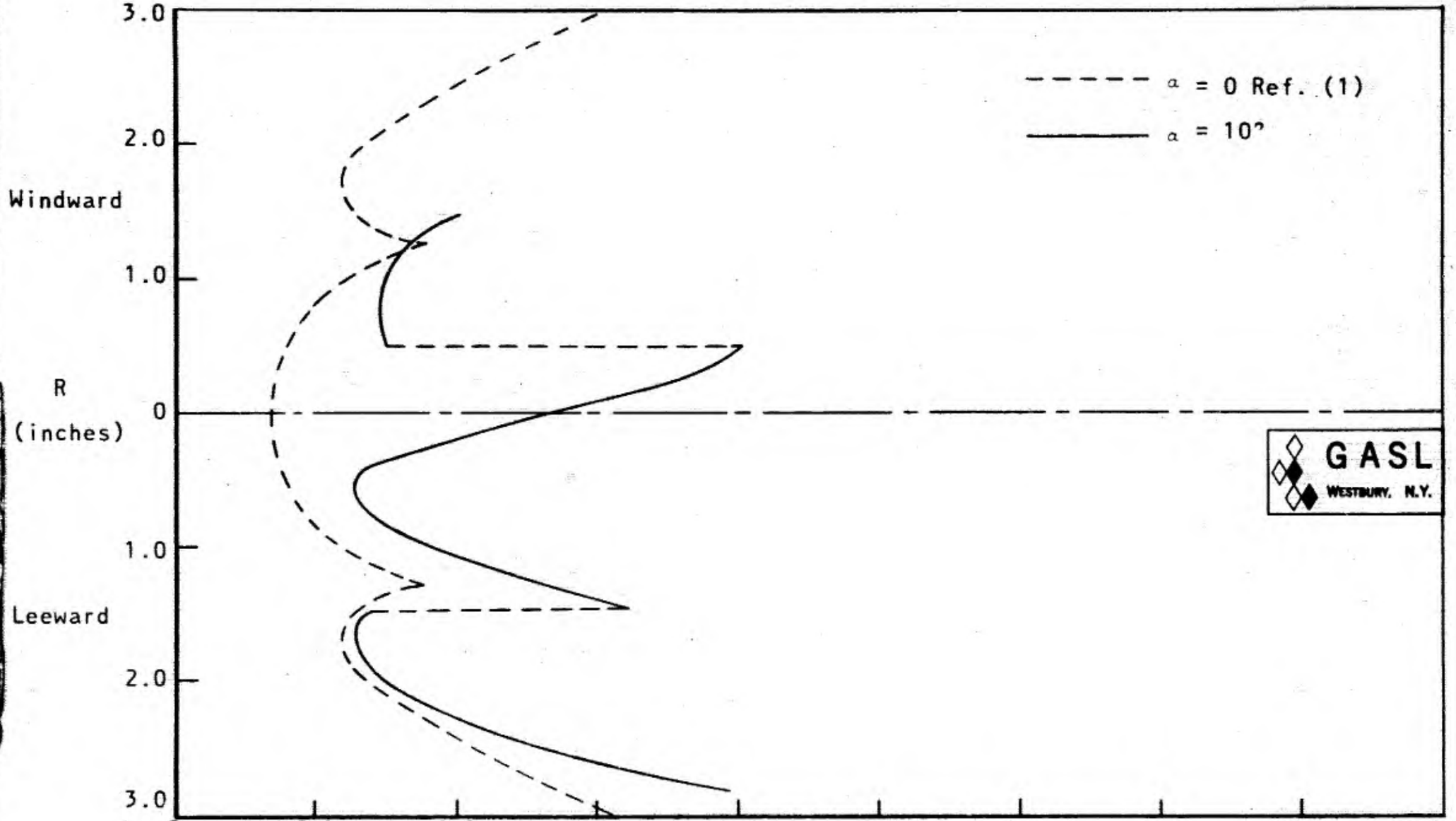

FIGURE 18: COMPARISON OF RADIAL PITOT PRESSURE PROFILES X/D = 1.25

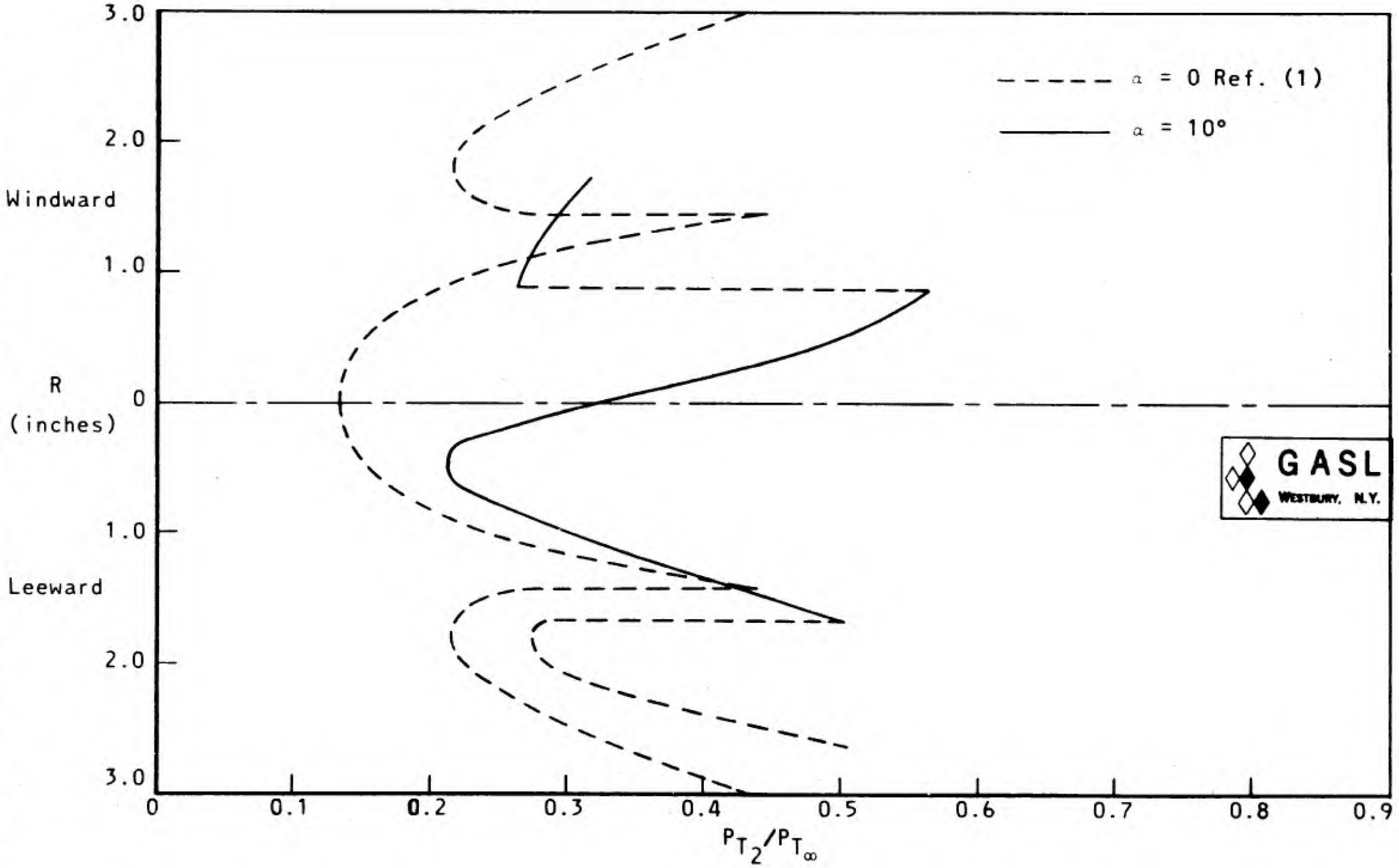

FIGURE 19: COMPARISON OF RADIAL PITOT PRESSURE PROFILES X/D = 1.75

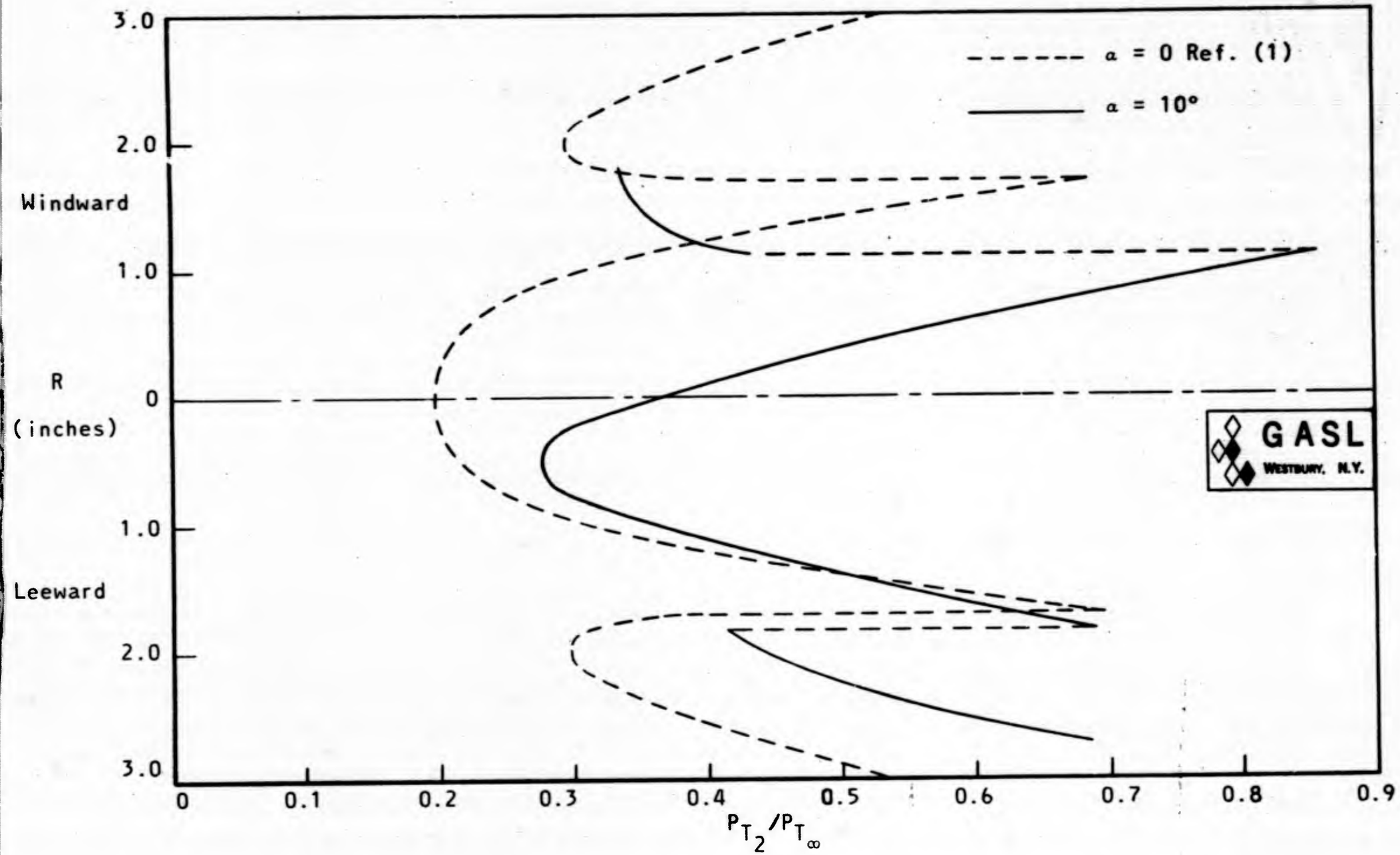

FIGURE 20: COMPARISON OF RADIAL PITOT PRESSURE PROFILES X/D = 2.25

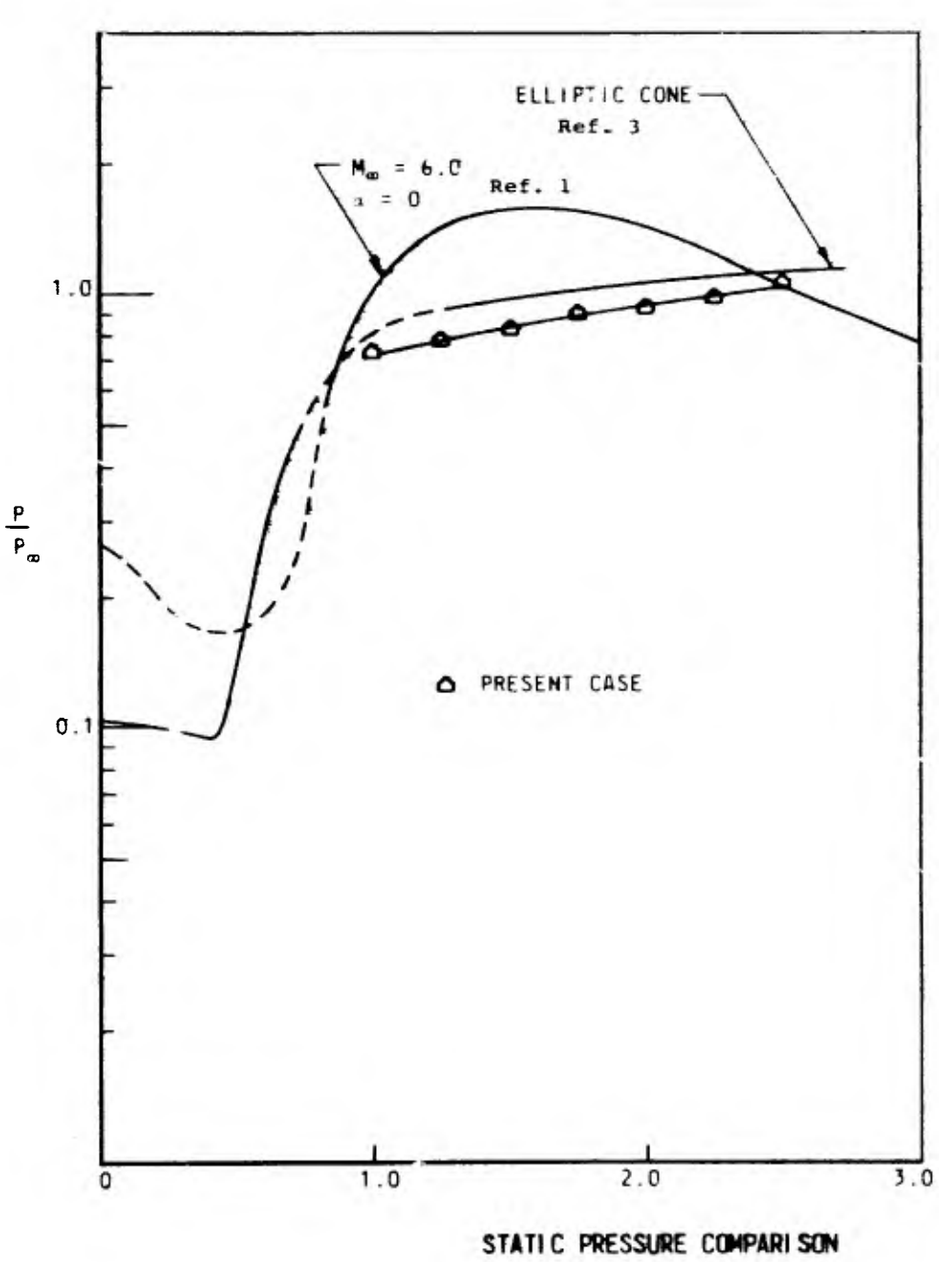

STATIC PRESSURE COMPARISON

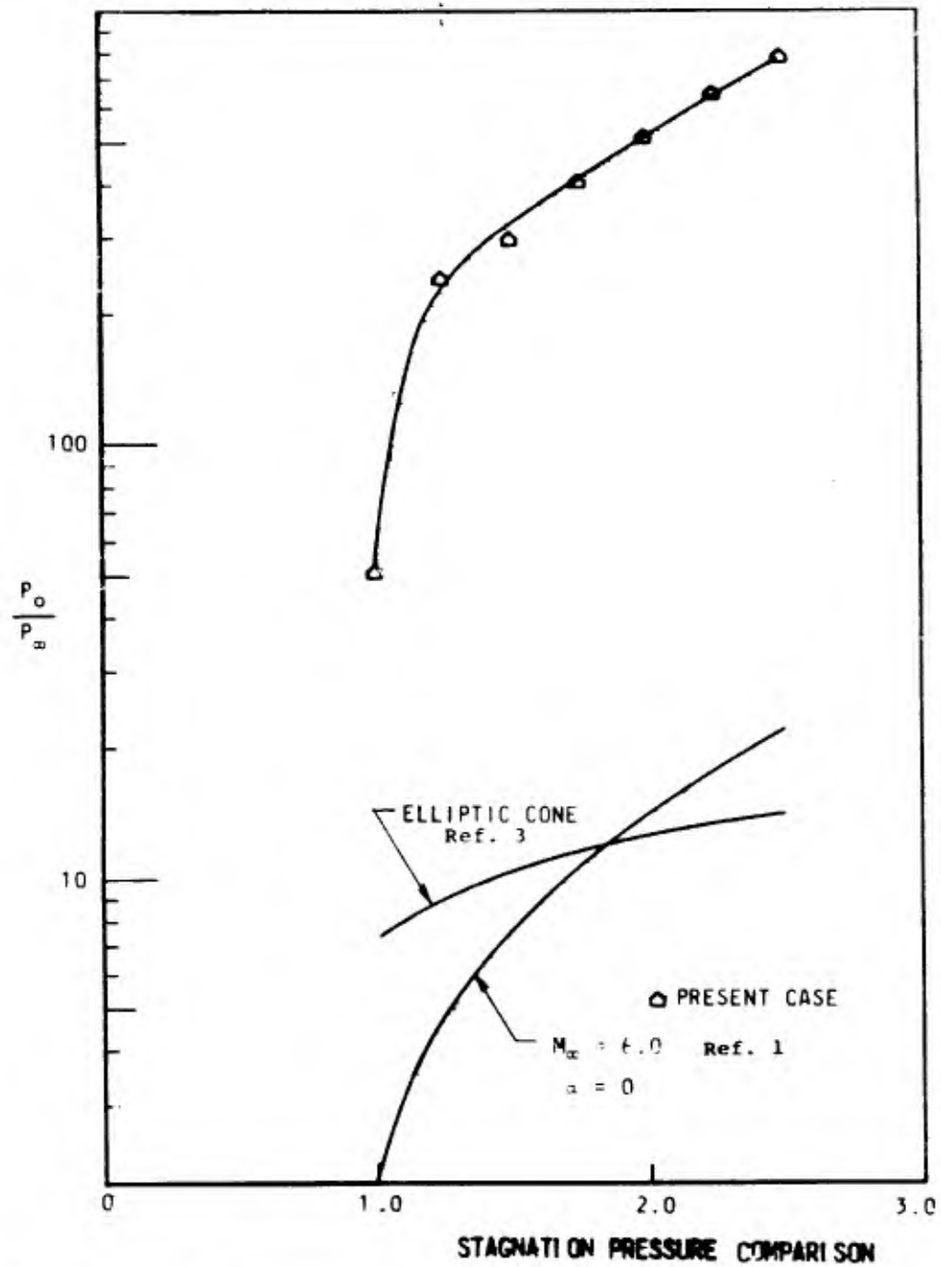

STAGNATION PRESSURE COMPARISON

FIGURE 21: NEAR WAKE PRESSURE DISTRIBUTION